PARAMETRIC INVESTIGATION OF WATER GAS SHIFT OVER Pd BASED CATALYSTS

by

Özge Ertem

B.S., Chemical Engineering, Yıldız Technical University, 2011

Submitted to the Institute for Graduate Studies in
Science and Engineering in partial fulfillment of
the requirements for the degree of
Master of Science

Graduate Program in Chemical Engineering

Boğaziçi University

2014

to my family

ACKNOWLEDGEMENTS

First of all, I would like to express my deepest gratitude to my supervisor Assoc. Prof. Ahmet Kerim Avcı, for his everlasting support, motivation and trust in me. It was a privilege for me to work with him during my thesis. Without his kind attitude and encouragement this study would have been a lot harder for me.

I would like to acknowledge my thesis committee Prof. Ramazan Yıldırım and Assoc. Prof. Hasan Bedir for devoting their valuable time to read and comment on my thesis. I am also thankful to Prof. Ahmet Erhan Aksoylu for his suggestions and encouragement during my experimental studies.

Heartfelt thanks goes to Hayri Onur Kavaklı, who understands me the best and stands by me in this period. His unique guidance and endless help taught me a lot during this work. Thanks to this thesis, I have gained a very valuable friend.

Special thanks to Bilgi Dedeoğlu, who always greets me with his huge smile and helps me patiently whenever I need. I would also like to thank Bilge Gedik Uluocak for her considerable efforts in SEM analysis conducted at Boğaziçi University Advanced Technologies Research and Development Center.

I would like to express my appreciation to Büşra Gürses and Sezin Sezen for their valuable friendships; their cheerfulness made my days in KB more enjoyable. Special thanks to Melek Selcen Başar for her support and motivation. I am also very grateful to Burcu Karagöz for being next to me; I wish her all the best in her new life.

Cordial thanks to nice members of KB 411, Merve Eropak, Ali Uzun, Cansu Yassı, Doğa Demirhan, Emre Demirel, Serhat Erşahin and Hazal Bal; I was very lucky to share the same working environment with these people. It was a real pleasure for me to work with all the other people in CATREL team.

I would like to acknowledge TÜBİTAK for granting me a scholarship during my master education.

Finally, I devote this thesis to my mother, father and my brother Caner. I always feel their endless love and support through my entire life. I am very lucky to have them.

ABSTRACT

PARAMETRIC INVESTIGATION OF WATER GAS SHIFT OVER Pd BASED CATALYSTS

The purpose of this study is to investigate WGS reaction over Pd based catalysts, cheaper alternatives of Au and Pt, and explore the impact of reactor structuring on CO conversion. The Pd based catalysts used in this research, which contains 1.5wt.% active metal, were prepared by incipient to wetness impregnation method with various types of support materials, including CeO_2, Al_2O_3 and TiO_2. The effects of reaction temperature and feed composition on WGS activity comparatively studied in conventional packed bed reactor and a packed microchannel reactor in the temperature and molar steam to carbon (S/C) ratio ranges of 250-325 °C and 1-5, respectively. Experimental studies revealed that among the prepared catalysts WGS activity, measured in terms of CO conversion, followed the order of Pd/CeO_2>$Pd\text{-}CeO_2/Al_2O_3$>Pd/TiO_2. CO conversion was improved at higher temperatures and molar steam to carbon ratios in the feed. Additionally, when compared with conventional fixed bed reactor, microchannel configuration involving less amount of catalyst exhibited better reactor productivity expressed in terms of per cent conversion per unit mass of catalyst. Scanning electron microscopy (SEM) analyses were conducted over CeO_2 and Al_2O_3 supported catalyst samples and uniform Pd dispersion was observed in both cases. SEM analysis on catalysts exposed to reaction detected no coke formation and agglomeration of Pd particles.

ÖZET

SU GAZI GEÇİŞİ REAKSİYONUNUN Pd BAZLI KATALİZÖRLER ÜZERİNDE PARAMETRİK İNCELENMESİ

Bu çalışmada, Au ve Pt'ye daha ucuz bir alternatif olan Pd bazlı katalizörler üzerinde su gazı geçişi reaksiyonunun davranışının incelenmesi ve reaktör geometrisinin CO dönüşümü üzerindeki etkisinin araştırılması hedeflenmiştir. Çalışmalarda kullanılan, ağırlıkça %1.5 aktif metal içeren Pd bazlı katalizörler CeO_2, Al_2O_3 ve TiO_2 gibi farklı destek malzemeleri kullanılarak emdirme yöntemi ile hazırlanmıştır. Reaksiyon sıcaklığının ve besleme akımı içeriğinin su gazı geçiş reaksiyonu üzerindeki etkisi sabit yatak reaktörde ve dolgulu mikrokanal reaktörde karşılaştırmalı olarak 250-325 °C sıcaklık aralığında ve 1-5 molar buhar/karbon oranı aralıklarında incelenmiştir. Deneysel çalışmalarda kullanılan katalizörler için CO dönüşümü cinsinden ifade edilen su gazı geçiş reaksiyonu aktivitesi sıralaması Pd/CeO_2>$Pd\text{-}CeO_2/Al_2O_3$>Pd/TiO_2 olarak belirlenmiştir. Reaksiyon sıcaklığı ve buhar/karbon oranındaki artış ile birlikte CO dönüşümünün arttığı gözlenmiştir. Sabit yatak reactor düzeniyle karşılaştırıldığında, dolgulu mikrokanal reaktörün daha az katalizör miktarı ile daha yüksek üretkenlik gösterdiği belirlenmiştir. Taramalı elektron mikroskopu (SEM) analizleri CeO_2 ve Al_2O_3 destek malzemesi içeren katalizörler için yapılmış ve her iki katalizör üzerinde Pd dağılımının homojen bir şekilde gerçekleştirildiği görülmüştür. Reaksiyon sonrası katalizörler üzerinde yapılan SEM analizlerinde ise herhangi bir karbon oluşumu ve Pd metal tanecik boyutunda büyüme gözlenmemiştir.

TABLE OF CONTENTS

ACKNOWLEDGEMENTS iv
ABSTRACT vi
ÖZET vii
LIST OF FIGURES x
LIST OF TABLES xiii
LIST OF SYMBOLS xiv
LIST OF ACRONYMS/ABBREVIATIONS xv
1. INTRODUCTION 1
2. LITERATURE SURVEY 4
2.1. Hydrogen Technology 4
2.2. Water Gas Shift Reaction 6
2.3. Water Gas Shift Catalysis 8
2.4. Water Gas Shift Reaction Mechanisms and Kinetics 17
2.5. Microchannel Reactors 20
3. EXPERIMENTAL WORK 23
3.1. Materials 23
3.1.1. Chemicals 23
3.1.2. Gases and Liquids 23
3.2. Experimental Systems 24
3.2.1. Catalyst Preparation System 24
3.2.2. Catalyst Characterization System 25
3.2.3. Catalytic Reaction System 25
3.2.4. Product Analysis System 28
3.3. Catalyst Preparation and Pretreatment 29
3.3.1. Preparation of Pd/CeO_2 Catalyst 29
3.3.2. Preparation of $Pd\text{-}CeO_2/Al_2O_3$ Catalyst 30
3.3.3. Preparation of Pd/TiO_2 Catalyst 31
3.3.4. Catalyst Coating on Microchannel Plates 31
3.3.5. Pretreatment 32

3.4. Reaction Tests 32
3.4.1. Blank Tests 32
3.4.2. WGS in Conventional Packed Bed Reactor 33
3.4.3. WGS in Microchannel Reactor 35
4. RESULTS AND DISCUSSION 37
4.1. WGS in Conventional Packed Bed Reactor 37
4.1.1. Catalyst Characterization 42
4.2. WGS in Packed Microchannel 46
5. CONCLUSIONS AND RECOMMENDATIONS 51
5.1. Conclusions 51
5.2. Recommendations 52
APPENDIX A: CALIBRATION OF MASS FLOW CONTROLLERS 53
APPENDIX B: CALIBRATION OF THE GAS CHROMATOGRAPHS 55
REFERENCES 58

LIST OF FIGURES

Figure 3.1. The Impregnation System. 25

Figure 3.2. Schematic Diagram of the Reaction System. ……... 26

Figure 3.3. H-type Steel Housing including Two Coated Plates and Catalytic Microchannel. 31

Figure 3.4. Schematic Diagram of the Conventional Packed Bed Reactor and Furnace System. 33

Figure 3.5. Packed Microchannel Configuration. 35

Figure 4.1. Effect of Temperature and S/C on CO Conversion over 1.5%Pd/CeO_2 Catalyst. …… 38

Figure 4.2. CO Content in the Product Stream during Reaction over Pd/CeO_2 at 325 °C. 39

Figure 4.3. CO Content in the Product Stream during Reaction over Pd/CeO_2 at 300 °C. 39

Figure 4.4. The Effect of Catalyst Support on CO Conversion. ……. 41

Figure 4.5. CO Content in the Product Stream during Reaction over Pd-CeO_2/Al_2O_3 at 300 °C. 42

Figure 4.6. Backscattering Electron (BSE) SEM Micrographs and Ce and Pd Mappings of Reduced Pd/CeO_2 Catalyst. 43

Figure 4.7. Backscattering Electron (BSE) SEM Micrographs and Ce and Pd Mappings of Reduced Pd-CeO_2/Al_2O_3 Catalyst. 44

Figure 4.8. Backscattering Electron (BSE) SEM Micrographs of Reduced and Reacted Catalysts. 45

Figure 4.9. The Catalyst Productivity in Conventional Packed Bed and Packed Microchannel Reactors at 300 °C. …… 47

Figure 4.10. The Catalyst Productivity in Conventional Packed Bed and Packed Microchannel Reactors at325 ˚C. ……. 47

Figure 4.11. CO Content in the Product Stream during Reaction over Pd/CeO_2 in Packed Microchannel at 300 °C. 49

Figure 4.12. CO Content in the Product Stream during Reaction over Pd/CeO_2 in Packed Microchannel at 325 °C. 49

Figure A.1. Calibration Curve of the Nitrogen Mass Flow Controller. ……... 53

Figure A.2. Calibration Curve of the Hydrogen Mass FlowController. …….. 53

Figure A.3. Calibration Curve of the Carbon Monoxide Mass Flow Controller. 54

Figure A.4. Calibration Curve of the Carbon Dioxide Mass Flow Controller. ... 54

Figure B.1. GC Calibration Curve for Nitrogen. 55

Figure B.2. GC Calibration Curve for Hydrogen. 55

Figure B.3. GC Calibration Curve for Carbon Monoxide. 56

Figure B.4. GC Calibration Curve for Carbon Dioxide. 56

Figure B.5. GC Calibration Curve for Methane. 57

LIST OF TABLES

Table 3.1.	Chemicals used for catalyst synthesis.	23
Table 3.2.	Specifications and the applications of liquids used in experiments.	23
Table 3.3.	Specifications and applications of the gases used. ……...	24
Table 3.4.	GC conditions for reactant and product analyses. ……	28
Table 3.5.	Reaction conditions for catalytic activity tests.	34
Table 3.6.	List of experiments on Pd based catalysts in conventional packed bed reactor. ……...	34
Table 3.7.	List of experiments on Pd based catalyst in packed microchannel reactor.	36
Table 4.1.	Product compositions (in dry basis) for 1.5%Pd/CeO_2 catalyst.	40
Table 4.2.	Product compositions (in dry basis) from WGS at 300 °C for 1.5%Pd-20%CeO_2/Al_2O_3 and 1.5%Pd/TiO_2 catalysts. …….	42
Table 4.3.	SEM/EDX results for the metal contents of the catalysts.	44
Table 4.4.	Product compositions (in dry basis) for 1.5%Pd/CeO_2 catalyst in packed microchannel. ……...	50

LIST OF SYMBOLS

D	Diameter of the housing (mm)
dp	Particle diameter (mm)
ID	Inner diameter of the reactor (mm)
L	Length of the housing (mm)
F_{CO}^{in}	Carbon monoxide inlet flow ($mol.min^{-1}$)
F_{CO}^{out}	Carbon monoxide outlet flow ($mol.min^{-1}$)
K_{eq}	Equilibrium constant of water gas shift reaction
Ox	Oxidized sites
P_i	Partial pressure of species i
r_{Pd}	Water gas shift reaction rate
Red	Reduced sites
T	Temperature
W	Width of the microchannel (mm)
W_{cat}	Catalyst weight (mg)
X_{CO}	Carbon monoxide conversion
ΔG	Gibbs free energy of the reaction
ΔH	Enthalpy of the reaction ($kJ.mol^{-1}$)
ΔH_{298}°	Standard enthalpy of the reaction ($kJ.mol^{-1}$)
υ_i	Flow rate of the species i ($ml.min^{-1}$)
σ	Adsorption sites of the metal
*	Active metal sites

LIST OF ACRONYMS/ABBREVIATIONS

AFC	Alkaline Fuel Cell
ATR	Auto-thermal Reforming
BSE	Backscattering Electron
DMFC	Direct Methanol Fuel Cell
DRIFTS	Diffuse Reflectance Infrared Fourier Transform Spectroscopy
EDX	Energy Dispersive X-ray Analysis
FC	Fuel Cell
FTIR	Fourier Transform Infrared
GC	Gas Chromatography
HPLC	High Pressure Liquid Chromatography
HTS	High Temperature Shift
LTS	Low Temperature Shift
MCFC	Molten Carbonate Fuel Cell
MFC	Mass Flow Controller
OSC	Oxygen Storage Capacity
PAFC	Phosphoric Acid Fuel Cell
PEMFC	Proton Exchange Membrane Fuel Cell
POX	Partial Oxidation
PROX	Preferential Carbon Monoxide Oxidation
PSA	Pressure Swing Adsorption
S/C	Steam to Carbon Ratio
SEM	Scanning Electron Microscopy
SOFC	Solid Oxide Fuel Cell
SR	Steam Reforming
TCD	Thermal Conductivity Detector
TPR	Temperature Programmed Reduction
W/F	Catalyst Weight to Feed Flow Rate Ratio

1. INTRODUCTION

The demand of energy is increasing faster in worldwide due to the rapid industrialization and population growth. As a result of the extended use of fossil fuels global CO_2 emissions increase drastically. Extensive studies have recently been carried out on looking for renewable resources to eliminate fossil fuels dependence. Unlike wind and solar energy, hydrogen can be stored and transported; thus hydrogen is considered to be the most effective energy carrier in the future. In particular, there is a progressive development in fuel cells, which can be used for transportation, primary power generation and distributed generation, and it is known that hydrogen is a vital fuel for the fuel cells (Chen *et al*., 2008).

The proton exchange membrane fuel cells (PEMFC) are the most promising electrochemical devices for stationary and vehicular applications, owing to their high power density, compactness and dynamic response characteristics (Lenite *et al*., 2011). Pure H_2 is the ideal source of energy for PEM fuel cells and it is supplied from catalytic partial oxidation or steam reforming of fossil or renewable hydrocarbons. One of the most critical issues in PEMFCs is the fuel cell anodes that be poisoned even by trace impurities of CO; therefore this component has to be removed to a level below 10 ppm. The water gas shift (WGS) reaction is an essential step to reduce CO content of the H_2 stream to an acceptable concentration before it is fed into fuel cell.

As a result of the advancements in fuel cell technology the interest towards WGS reaction has increased. Since conventional catalysts used in WGS reaction are not applicable for small scale, on-board applications, studies are focused on developing novel catalysts, which can meet the requirements for achieving feasible, effective and stable operation. In this respect, noble metal catalysts offer several advantages such as exhibiting high activity at wide temperature ranges, resistance towards start up-shut down cycles and no need of activation prior to use. Platinum group metals, especially Pt and Au, are widely investigated for the WGS reaction and satisfactory activities are reported for both of these catalysts (Deshpande *et al*., 2010; Lenite *et al*., 2011). However the high prices of Pt and Au, 1469 dollars/ounce Pt and 1257 dollars/ounce Au (BASF Catalysts, 2014), make them

infeasible for use in WGS from the cost point of view, and, as a result, cheaper alternatives start to become attractive. At this point Pd, which is cheaper than other platinum group metals (845 dollars/ounce Pd (BASF Catalysts, 2014)), can be considered as an alternative metal in WGS catalysts. Studies indicate that, the activity of Pd catalysts for WGS can be improved by formation of alloys between Pd and other metals (Colussi *et al*., 2014).

In addition to high and stable catalytic activity, compactness is another important criterion for WGS unit in fuel cell applications. Industrially WGS reaction takes place in two steps due to its thermodynamic limitations; therefore with traditional reactor systems the WGS unit is expected to be the largest component in fuel processor. Catalytic microchannel reactors can be a promosing solution for the high space demands of the WGS reactor. When compared with conventional packed bed reactors, microchannels provide faster and uniform heat transfer rates, which is crucial for the WGS reaction. High heat transport rates enable better distribution of heat to the catalyst bed at low temperatures at which WGS is hindered by reaction kinetics. Moreover, the exothermic heat that elevates the reaction temperature and limits the conversion due to infavorable thermodynamic behavior can be removed fastly. Consequently, the possibility of running WGS at isothermal conditions can be realized. In addition to these benefits, microchannel reactors decrease the weight and volume of the reactor to a great extent due to their very high surface area-to-volume ratios (ca. 10000/50000 m^2/m^3) which are notably higher than those of conventional units (up to ca. 1000 m^2/m^3) (Kiwi-Minsker and Renken, 2005).

In this work low temperature WGS reaction is studied over Pd based catalysts supported on various oxide supports in the context of a parametric plan. The effect of reaction temperature, feed composition and the catalyst support are investigated at conventional packed bed and microstructured reactor configurations. In addition the structural changes on catalyst surface after reaction are examined by scanning electron microscopy (SEM) analysis.

This study mainly consists of five sections. Chapter 2 includes general literature survey about fuel cell technology and hydrogen production, WGS reaction and experimental studies over various types of catalysts and mechanism of WGS on noble metal catalysts. In Chapter 3, techniques and procedures used for catalyst preparation and

catalytic activity tests are explained in detail. Chapter 4 involves results and discussions obtained from experimental studies and finally major conclusions and recommendations for future works are given in Chapter 5.

2. LITERATURE SURVEY

2.1. Hydrogen Technology

For many years hydrogen economy has attracted a great interest since hydrogen has been widely used as a raw material for industrial applications, such as ammonia synthesis, the breaking down of heavier crude oils and the removal of sulfur (Chen and Jheng, 2007). The demand of hydrogen is expected to increase in the future for clean energy generation. Unlike wind and solar energy hydrogen can be stored and transported. In addition, for the characteristics of high power density and zero greenhouse gas emission, hydrogen is considered to be the most effective energy carrier and a vital fuel for fuel cells (Chen *et al.*, 2008).

The fuel cell technology, an environmentally friendly and high efficiency process, is regarded as one of the renewable energy source for power plant and transport applications. Fuel cells are electrochemical devices which convert chemical energy of the fuel directly into electrical energy without Carnot efficiency limitations (Galvita *et al*., 2008). They consist of an electrolyte layer between anode and cathode electrodes. Over the anode electrode hydrogen from the fuel decomposes into positive and negative ions. Positive ions flow through the electrolyte and at the cathode electrode they combine with an oxidant and produce water, while negative ions move to the cathode side through an external unit and create an electrical circuit. Depending on the electrolyte and the fuel type, fuel cells can be categorized as follows (Kirubakaran *et al*., 2009):

- Proton exchange membrane fuel cell (PEMFC)
- Alkaline fuel cell (AFC)
- Phosphoric acid fuel cell (PAFC)
- Molten carbonate fuel cell (MCFC)
- Solid oxide fuel cell (SOFC)
- Direct methanol fuel cell (DMFC)

Compared to the other fuel cell types, PEMFCs are considered as the most suitable systems to generate power for residential units and transport applications, due to their high power density, low operating temperature, mechanical robustness, compactness, long stack life and quick start-up characteristics (Lenite *et al*., 2011). The most successful fuel cell systems work with pure hydrogen fuel and they produce only water as a by-product; thus hazardous gas emission is eliminated. For this reason, efficient and feasible hydrogen generation is an important issue in order to enhance the utilization and the applications of the fuel cells.

Recently hydrogen is extensively produced by natural gas (48%), followed by oil (30%) and coal (18%) and only 4% of hydrogen production is supplied by water electrolysis (Noor *et al*., 2014). Steam reforming (SR), auto-thermal reforming (ATR) and partial oxidation (POX) of hydrocarbons are conventional ways to produce hydrogen and they can be generalized as expressed below. Among these three production technologies, steam reforming of methane is the most preferable hydrogen production process in industry since it operates at lower temperatures and produces the highest H_2:CO ratio (~ 3:1) (Holladay *et al*., 2009; Trimm, 2005).

SR : $$C_mH_n + mH_2O \leftrightarrow mCO + \left(m + \frac{1}{2}n\right)H_2 \qquad \Delta H>0 \qquad (2.1)$$

POX: $$C_mH_n + \frac{1}{2}mO_2 \leftrightarrow mCO + \frac{1}{2}nH_2 \qquad \Delta H<0 \qquad (2.2)$$

ATR: $$C_mH_n + \frac{1}{2}mH_2O + \frac{1}{4}mO_2 \leftrightarrow mCO + \left(\frac{1}{2}m + \frac{1}{2}n\right)H_2 \qquad \Delta H\leq 0 \qquad (2.3)$$

The product streams of these processes contain high amounts of CO (8-10% by volume) as a by-product. Fuel cells which operate at high temperatures can tolerate high concentrations of CO and CO_2. On the other hand, at low-temperature fuel cells, like PEMFC, irreversible adsorption of CO takes place on the surface of Pt electrode and blocks the active sites. Therefore, it is important to reduce CO content of the H_2 rich stream to ppm levels (<10-20 ppm) before it is fed to the fuel cell unit (Galvita *et al*., 2007).

Theoretically, there are several approaches that can be used to remove CO from H_2 rich gases to acceptable concentrations for PEMFC applications. One of the method is membrane separation in which H_2 permeates through a Pd-Ag membrane and pure H_2 gas can be obtained. However, it requires a high differential pressure difference between the two sides of the membrane and high temperature, which elevates the cost and restricts the utilization of membranes. Pressure Swing Adsorption (PSA) is another option for CO removal process. Adsorptive material like zeolite is employed, which adsorbs the undesired gas component at high pressure. The pressure is lowered then to desorb adsorbed compound, thus the system requires two parallel units and a reliable control to switch cyclically (Lenite *et al*., 2011).

Since low operating pressure and compactness are important for PEMFC applications on vehicles and portable devices, apart from the approaches mentioned above, recently water gas shift (WGS) reaction is the most promising way to reduce the CO concentration to trace levels which is subsequently followed by preferential CO oxidation (PROX) or selective CO methanation as a final purification step (Lenite *et al.*, 2011).

2.2. Water Gas Shift Reaction

The WGS reaction has been an important step in industrial production of hydrogen since 1940s and according to the recent reports, about 10% of the worldwide yearly energy consumption is estimated to be derived from the WGS by 2030 (Noor *et al.*, 2014). In this process, as shown in Equation 2.4, water in the form of steam reacts with CO from syngas and converts it into CO_2, while simultaneously produces additional hydrogen (Jacobs *et al*., 2003).

$$CO+H_2O \leftrightarrow CO_2+H_2 \qquad \Delta H°_{298} = -41.1 \text{ kJ.mol}^{-1}, \Delta G°_{298} = -28.6 \text{ kJ.mol}^{-1} \qquad (2.4)$$

The crucial role of the WGS is to adjust the H_2/CO ratio to the desired value for Fischer-Tropsch and methanol synthesis. Furthermore it is an essential process to produce CO free hydrogen, which is very important for fuel-cell applications and ammonia synthesis, due to the poisonous effect of CO on iron catalyst used in ammonia production and anodic platinum electrode of the fuel cells (Soria *et al*., 2013).

The WGS is moderately exothermic, reversible reaction and its equilibrium constant, which can be calculated by Equation 2.5, decreases with increasing temperature (Kolb *et al*., 2005). High CO conversions are promoted at lower temperatures, however in that case the reaction rate is limited by kinetics. In order to achieve high CO conversions by high reaction rates and reduced reactor volumes, traditionally WGS reaction is performed in two steps. The first step, high temperature shift (HTS), operates at 350-450 °C temperature range and since it uses the advantage of the favorable kinetics, significant amount of CO can be converted with minimal catalyst requirements. For instance, syngas generated from autothermal reforming contains 8-10% CO by volume and this value can be reduced to 3-4% by HTS. The second step, low temperature shift (LTS), operates at thermodynamically favorable conditions (at 200-300˚C) and can reduce the CO content down to 0.5-1% (Önsan, 2007; Ladebeck and Wagner, 2003).

$$K_{eq} = \exp\left(\frac{4577.8}{T(\mathrm{K})} - 4.33\right) \tag{2.5}$$

In contrast with temperature, pressure has a negligible effect on WGS, since the reaction is equimolar there is no volume difference between reactants and products (Smith *et al*., 2010). Ladebeck and Wagner (2003) indicate that increasing the pressure from 3 to 30 atm has almost no effect on CO conversion.

The steam/gas ratio is another crucial parameter at WGS reaction. Increasing the molar steam to dry gas (effluent gas from the reforming process includes CO and CO_2) ratio promotes forward reaction rate and higher values of CO conversions could be obtained. On the other hand, utilizing too low steam/dry gas ratio might result in catalyst deactivation due to the coke formation. Too high values of steam/dry gas ratios elevates energy costs and is not preferable for process economy (Ratnasamy and Wagner, 2009). It is reported that, increasing the steam/dry gas ratio from 0.25 to 0.75 raise equilibrium temperature by 100 °C. This means favorable kinetics and thermodynamics for high CO conversions could be achieved at 100 °C higher temperature and it provides an important reduction in reactor size (Ladebeck and Wagner, 2003).

Methanation reaction, which is described as Equation 2.6, should be also considered during WGS process, since it might take place under the WGS reaction conditions and it consumes valuable amount of H_2, thus decreases the overall H_2 production (Kolb *et al.*, 2005).

$$CO+3H_2 \rightarrow CH_4+H_2O \qquad \Delta H_{298} = -283.6 \text{ kJ/mol} \qquad (2.6)$$

Due to the fact that the thermodynamic nature of the WGS reaction constrains the equilibrium conversion at high temperatures and favors the low temperatures, the WGS reaction rate is relatively slow and hence the reactor volume is large when compared to other reactions in overall fuel processor (Choi and Stenger, 2003). This is an important drawback of the WGS reaction when used in fuel cell applications. In order to reduce the volume and weight of the shift reactors studies have been focused on the development of advanced novel catalysts for WGS to obtain adequate activity at optimal conditions.

2.3. Water Gas Shift Catalysis

The WGS reaction process can be operated in the presence or absence of a catalyst. The non-catalytic WGS reaction occurs in an environment of water under supercritical conditions (Chen and Jheng, 2007). Sato and coworkers (2004) conducted experiments in supercritical water where CO/H_2O ratio was 0.03 at 653-713 K temperature range and observed that for all the experiments CO conversion values were below 11% and the reaction rate was relatively slow compared the conventional catalytic processes.

In general, the WGS reaction is carried out in the presence of a catalyst. For HTS, conventionally iron-chromium based catalysts are employed. These catalysts performed well at high reaction temperatures and are not sensitive to sulphur; in addition depending on the reaction temperature they have a life time of 3-5 years. However they are not active at temperatures below 350 °C. Their another drawback is after exposure to air, due to their pyrophoric feature, they require a pre-treatment before being reused; therefore they should be re-reduced and stabilized by surface oxidation by using an inert gas with a low concentration of oxygen (Trimm, 2005; Callaghan, 2006).

Typical Fe_2O_3-Cr_2O_3 catalysts contain about 80-90wt% Fe_2O_3, 8-10wt.% Cr_2O_3 and are balanced with promoters or stabilizers like copper oxide, Al_2O_3, MgO, ZnO etc. The role of the Cr_2O_3 and Al_2O_3 is to stabilize the material, prevent sintering and the loss of surface area of the active phase iron oxide. Moreover Cr_2O_3 can also increase the catalytic activity of Fe_2O_3 (Ratnasamy and Wagner, 2009). The important thing for this process is maintaining the interchange between different oxides of iron, since formation of metallic iron may result in exothermic methanation reaction, reduce the selectivity and cause the catalyst deactivation. Therefore careful control of temperature, H_2O/H_2 and CO_2/CO ratios are needed (Önsan, 2007; Trimm, 2005).

The performance of the iron-chromium based catalysts can be enhanced by the addition of small amount of noble metals or base metals (Önsan, 2007). Rhodes and coworkers (2002) investigated the activity of Fe_3O_4/Cr_2O_3 catalysts that were promoted by various types of metals in the temperature range from 350 to 440 °C. It was found that the addition of 2wt.% Hg, Ag, Ba, Cu and Pb increased the activity, while addition of boron showed no significant effect on activity of Fe_3O_4/Cr_2O_3 catalyst. The possible reason of these observations is due to the fact that the promoters, which have different ionic sizes from Fe^{+2}, join into Fe_3O_4 lattice and affect the electronic nature of the iron, hence influence the activity of the catalyst.

For the catalytic LTS case, catalysts usually consist of different compositions of copper, zinc oxide and alumina. Typical commercial LTS catalysts contain about 33% (by weight) CuO, 34% ZnO and 33% Al_2O_3. As copper metal crystallites act as active sites, ZnO provides structural support and also protects copper from sulphur poisoning. Alumina, an inactive component, helps dispersion, enhances the strength of the pellet and minimizes pellet shrinkage (Smith *et al.*, 2010; Rhodes *et al*., 1995). Copper based catalysts are generally preferred for industrial LTS, due to their higher selectivity, higher activity and fewer side reactions at high pressures (Amadeo and Laborde, 1995).

Choi and Stenger (2003) conducted performance tests over commercial $Cu/ZnO/Al_2O_3$ catalysts for methanol fuel processors for fuel cell applications in the temperature range between 120 to 250 °C. They investigated the effect of H_2O/CO ratio on CO conversion and reported that at constant temperature CO conversion increased with

increasing H_2O/CO ratio. For instance; at 220 °C when the value of H_2O/CO was 1:1, 70% CO conversion was obtained while almost 85% CO conversion was achieved when this value was increased to 2. They also performed deactivation tests over Cu/ZnO/Al_2O_3 catalyst for 250 h with various feed and operating conditions and it was found that over 250 h the activity loss of the catalyst for WGS was about 10%.

Instead of alumina, several oxides have been investigated as a support material for copper based catalysts and it was reported that the activity of the catalyst was also influenced by the kind of support. While Al_2O_3, MgO and CeO_2 supported copper-zinc oxide catalysts showed high activity, SiO_2-Al_2O_3, SiO_2-MgO and β-zeolite supported catalysts showed less activity at temperatures between 423-523 K. Among the prepared catalysts the most effective one was 4%Cu-5%ZnO supported on AlO8 (a type of Al_2O_3). This catalyst was compared with conventional CuO/ZnO/Al_2O_3 with the weight ratio 43:49:8 and it was indicated that, despite the conventional catalysts' copper content larger than the Cu-ZnO/AlO8, the activity per copper content is higher than the conventional oxide catalyst (Yahiro *et al.*, 2007).

Chen *et al.* (2008) performed parametric studies over commercial iron based HTS catalyst and copper based LTS catalyst. When the effect of residence time was investigated, it was seen that in either case increasing residence time enhanced the CO conversion and the ideal residence time was found to be 0.09 s. At HTS, the maximum CO conversion was achieved at 500 °C with 90%, while for LT case the optimum temperature was 200 °C, where the CO conversion was 93%. Furthermore increasing H_2O/CO ratio improved the CO conversion and especially for HTS, increasing reaction temperature promoted the reaction significantly at high H_2O/CO ratios. During WGS reaction measured H_2 concentrations were higher than CO_2. It was proposed that the existence of water decomposition reaction was the reason of this case and high temperatures triggered this reaction more.

Despite their ability of converting most of the CO remaining coming from the product stream of HTS, copper-based catalysts have several drawbacks which limit their utilization at mobile applications. The Cu-Zn-Al catalysts are unstable at temperatures above 300 °C, since active copper particles tend to sinter due to surface migration. During

activation careful control of temperature is also required because the reduction of the catalyst is highly exothermic. Additionally, these catalysts show highly pyrophoric feature at activated state if they are exposed to air, and they are not applicable for shut down-start up cycling at vehicular applications, because the active site of the catalyst is irreversibly deactivated by condensed water during quenching (Trimm, 2005; Kušar *et al.*, 2005).

For fuel processing applications, especially at compact fuel cell operations, reducing the size and weight of the LTS reactor is a crucial issue, which requires significant engineering and control strategies (Boaro *et al.*, 2008). In order to overcome thermodynamic and kinetic limitations of WGS reaction and operate at feasible conditions to achieve adequate activity, studies have been focused on developing precious metal supported catalysts. Ideal catalyst for fuel cell grade hydrogen production should be non-pyrophoric, resist in cycles of rapid heating and cooling and do not need to pre-reduction treatment. When compared to conventional WGS catalysts, precious metal catalysts show faster high temperature kinetics and they do not require activation prior to use and no degradation occurs when they are exposed to air. For this reason numerous studies have been carried out to develop effective catalyst for WGS by choosing the most appropriate precious metal (Cornaglia *et al.*, 2011; Soria *et al.*, 2013).

Many metals have been studied as an active component of the WGS catalyst. Au based catalysts have been relatively regarded as an appropriate candidate for CO removal owing to their low cost compared to other noble metals, such as Pt and Rh, and significant activity on WGS reaction at low temperatures when Au is deposited as nano-sized particles on metal oxides (Lenite *et al.*, 2011). On the other hand, Au based catalysts' activity is largely influenced by the catalyst preparation conditions and high metal loading (~5wt.%) is required, which is not feasible for large scale operations. Hence, various formulations of catalysts, which contain platinum group metals, have been investigated to obtain satisfying catalyst properties (Shinde and Madras, 2012).

In addition to nature of the metal, the support material also plays a crucial role on WGS activity. The physical and chemical characteristics of the metal and support, and their interaction at the interface influence the adsorption properties of the catalyst (Roh *et al.*, 2012). Cerium oxide (ceria) supported precious metal catalysts are important examples

for the significance of the metal-support interaction. Ceria based catalysts have been widely employed for oxidation and hydrogenation reactions because of ceria's high oxygen storage capacity. Ceria stores oxygen under oxidizing conditions and releases it under reduction conditions and promotes the reaction, while in the meantime improves the dispersion of the metal and stabilizes the catalyst (Li *et al.*, 2000; Bunluesin *et al.*, 1998).

Shinde and Madras (2012) suggested that reducibility and activity of CeO_2 could be also enhanced by using the effect of ionic substation of transition group metals. Cu-Ni and Cu-Fe modified CeO_2 catalysts were prepared by sonochemical method and complete CO conversion was obtained for Cu-Ni modified CeO_2 catalyst at 320 °C and 380 °C for Cu-Fe modified CeO_2. The reason for lower conversion of Fe modified catalyst was attributed to oxidation of Fe metal which could not stabilize the CO adsorption. It was indicated that the reaction stream included high fraction of water vapor thus the CO_2 adsorption and reverse WGS reaction were suppressed.

Zheng *et al*. (2005) pointed out that at the reactions involving ceria based catalysts, the preparation of CeO_2 crucially affected the catalyst activity. In this study CeO_2 was prepared by thermal decomposition of cerium nitrate ($Ce(NO_3)_3.6H_2O$) for 4 hours at 400, 500, 600 and 700 °C in air. It was observed that at 700˚C the crystallite size became much larger and irregular than other three samples. For the CuO/CeO_2 catalyst it was seen that calcination at temperatures above 600 °C caused rapid growth of crystallite size and phase separation between CuO and CeO_2, which reduced the catalytic activity.

Andreeva and coworkers (2002) studied ceria supported Au catalyst, which was prepared by deposition-precipitation method. When the effect of the Au loading was investigated it was seen that the activity increased with increasing Au percentage of the catalyst. It was also reported that the optimum catalyst sample was 3wt.%Au/CeO_2, which showed the highest stability after 3 weeks of operation. Surprisingly it was observed that under reaction conditions Au particles tended to decrease and it was thought that it was a result of the strong interaction between the ceria surface and the Au particles, thus high and stable catalyst activity was achieved.

Lenite *et al.* (2011) compared the activity of Au based catalysts supported on CeO_2 and Al_2O_3. It was indicated that (α-γ) Al_2O_3 was weak active support for WGS since only 30% CO conversion could be obtained, while with CeO_2 support the catalytic activity was improved and the conversion values closer to equilibrium curve were attained. The catalysts were synthesized by deposition-precipitation method and it was reported that the catalyst activity was also influenced by catalyst preparation conditions such as pH and the molarity of the Au precursor solution.

Zirconia (ZrO_2) can be alternative catalyst support for WGS reaction owing to its physical and chemical properties which affects the CO adsorption and metal-support interaction in a positive way. A detailed comparative study has been conducted by Boaro *et al.* (2009) by using pure ZrO_2 and CeO_2-ZrO_2 mixed oxide as a support material for Au and Pt based catalysts. It was observed that Au based catalysts supported on pure ZrO_2 exhibited higher activity than CeO_2-ZrO_2 mixed oxide support. The case was different for Pt based catalysts, since the similar activity was reported for both ZrO_2 and CeO_2-ZrO_2 supported catalysts which was prepared from Pt nitrate precursor, while for the Pt chloride precursor ZrO_2 supported catalyst exhibited better activity. It was indicated that the enhanced catalytic activity using nitrate precursor was related with the smaller Pt crystallites and high metal dispersion. At low temperatures Au catalysts showed significant conversion (20-50%) and as the temperature increased the conversion increased smoothly. On the contrary, over Pt based catalysts, conversion remained below 20% till 523 K and increased sharply and approached equilibrium value at 573 K.

The stability of the catalyst is as crucial as the catalytic activity during prolonged use, therefore this factor should be also carefully considered for the development of effective catalysts for FC applications. Au based catalysts are highly sensitive to the storage and operation conditions; hence in terms of robustness Pt based catalysts have an advantage over Au based ones (Ratnasamy and Wagner, 2009). Buitrago *et al.* (2012) studied the Pt based catalysts supported on activated carbon with different ceria loadings for LT-WGS. The Pt content of the catalysts was fixed at 1 wt.%. It was reported that while Pt/C catalyst was inactive for WGS reaction, Pt supported on C with 40% CeO_2 loading showed higher than 70% CO conversion at 573 K, which is higher than the activity

of Pt/CeO_2, and at this temperature no deactivation was detected under reaction conditions for 120 hours.

Although it is widely reported that Pt/CeO_2 is one of the most promising catalyst for LT-WGS, it was also reported that under real reformate conditions these catalysts also undergo deactivation. Zalc *et al.* (2002) investigated the deactivation phenomena on Pt/CeO_2 catalysts for realistic conditions and they observed rapid deactivation rate, 0.008 h^{-1}, which was independent of temperature. It was suggested that this case might be valid for all noble metal/ceria systems, since in the presence of high fraction of hydrogen in the feed results in irreversible over-reduction of the support, which might be the reason of the rapid deactivation. When the hydrogen was not present in the feed, the lower deactivation coefficient (0.002 h^{-1}) was observed.

As a response to the study of Zalc *et al.* (2002), Wang and coworkers (2002) pointed out that the loss of metal surface area was responsible for the deactivation of ceria supported catalysts. Pd/CeO_2 and Pt/CeO_2 catalysts were employed for the aging tests. As the reaction temperature was raised from 523 K to 673 K and reduced to initial temperature again, CO conversion dropped markedly. An attempt of regeneration of the catalyst under O_2 flow could not restore the initial conversion, which contradicts with the study of Zalc *et al.* (2002). By CO adsorption uptakes, significant decrease in Pd dispersion was detected. The case was valid for Pt based catalyst too, but the rate of deactivation was slower. The authors suggested that it was possible to develop stable ceria supported catalysts for WGS reaction by using promoters for maintaining metal surface area.

Kim *et al.* (2009) examined the WGS reaction over ceria promoted Pt catalysts supported on various materials under severe reaction conditions. Among the tested catalysts $Pt\text{-}Ce/TiO_2$ catalyst exhibited higher activity than the CeO_2, ZrO_2, Al_2O_3 and SiO_2 supported catalysts, especially at low temperatures. The maximum activity was observed when Ce/Pt molar ratio was 5 and with increasing Ce/Pt value the activity decreased. The stability of $Pt\text{-}Ce/TiO_2$ was also studied for the cyclic and start-up/shut-down operations and the stable catalytic performance was obtained for both of the cases.

Cornaglia *et al.* (2011) proposed a novel Rh based catalyst supported on La_2O_3-SiO_2 support for WGS. The loading of the Rh and La_2O_3 were 0.6wt% and 27wt% respectively. Kinetic studies at between the temperatures 598 and 723 K and H_2O/CO=3 ratio revealed that Rh/La_2O_3-SiO_2 exhibited higher activity and stability than Rh/La_2O_3, and constant CO conversion was obtained for at least 50 h, while no methanation was observed. It was also indicated that the synthesized catalyst was more active than the Fe, Cu and Pt based commercial catalysts reported in the literature.

According to the study, which compares the catalytic performance of four Pt group metals supported on ceria and Al_2O_3, the catalyst activity for WGS followed the order of Pt>Rh≈Ru>Pd (Panagiotopoulou and Kondarides, 2005). In spite of the fact that Pt supported ceria seem to be the most active catalyst for LT-WGS, issues related with its instability under fuel processing conditions lead investigators to develop more stable, active and also cost effective materials. At this point Pd, which is relatively more abundant and cheaper than Pt and Rh, attracts attention as a possible active metal for LT-WGS catalysts (Colussi *et al.*, 2014).

The comparative study of ceria based Pd and Pt catalysts for WGS reaction was conducted by Deshpande and coworkers (2010). The solution combustion method was applied for catalyst preparation, hence high ionic dispersion of the active metals and nanometer sized crystallites were obtained. When the feed stream consisted of N_2, CO and steam, at 275 °C Pt catalyst with %1 loading exhibited 90-95% CO conversion, while Pd catalyst showed activity close to Pt catalysts' at higher temperatures. Increasing substitution to 2% did not affect the reactivity, whereas in the presence of CO_2 and H_2 in the feed, increasing metal loading enhanced the catalytic activity. At this condition the maximum CO conversion was 88% with Pt catalyst, while with Pd catalyst this value was only 40%.

The catalytic activity of the metallic Pd can be enhanced by the formation of alloys between Pd and other metals. For instance it was demonstrated that under realistic process conditions, CeO_2 supported PdZn catalyst could be an alternative to commercial CuZnAl catalyst, since it exhibited highly stable behavior under start-up/shut-down cycles and resisted to liquid water. Moreover, after these cycles the complete recovery of the catalyst

activity could be achieved by in situ reduction (Colussi *et al.*, 2014). In another study, it was reported that PdZnAl type catalysts also showed significant activity and stability for WGS, comparable to a commercial Pt-based catalysts (Dagle *et al.*, 2008).

Fe_2O_3 has been found to be an effective oxide promoter for Pd/ceria catalysts for WGS. The study of Wang and Gorte (2003) revealed that the rate and the activation energy of Pd/ceria increased significantly with the addition of Fe_2O_3. At 473 K 1wt.%Pd/ceria catalyst promoted with 2wt.% Fe_2O_3 showed almost 8 times higher reaction rate than pure Pd/ceria catalyst. The role of the promoters had been thought to be to affect the barrier for oxygen transfer from ceria to Pd.

Kugai *et al.* (2011) carried out experiments over ceria supported Pd-Cu bimetallic catalyst for LT-WGS reaction. The catalysts were prepared by incipient to wetness impregnation method and Pd and Cu loadings were 1wt.% and 5wt.%, respectively. Strong interaction was observed between Pd and Cu by oxygen storage capacity (OSC) and temperature programmed reduction (TPR) measurements, which allowed to bimetallic catalyst to be more resistant towards oxidation. It was also demonstrated that the existence of Cu facilitated the CO_2 desorption from Pd catalyst. For Pd-Cu catalysts at 260 °C, 49% CO conversion was reported, while the presence of H_2 in the feed reduced this value to 21%. It was suggested that the addition of small amount of O_2 (~%1) to the feed at very short contact time enhanced CO conversion and H_2 production, since it oxidizes the small amount of CO and provides available catalyst surface sites thus more CO could react with H_2O.

Al_2O_3 supported Pd catalyst, which shows very low CO conversions at WGS reaction, can be promoted by the addition of CeO_2 and K_2O_3 and remarkable improvement of the catalytic activity could be achieved. Lee and Chen (1998) synthesized Pd-CeO_2/Al_2O_3 catalyst consisted of 0.4wt.% Pd and 16.8wt.% CeO_2 and CO conversions above 30% was obtained. The activity was further improved by the addition of K_2O_3 since it increased the basicity of the catalyst and suppressed the binding strength between Pd surface and the adsorbed species.

2.4. Water Gas Shift Reaction Mechanisms and Kinetics

Despite the WGS is an old industrial process, there is still no consensus on the mechanism of the reaction. Mainly two different mechanisms are proposed and both of them are supported by many researches (Amadeo and Laborde; 1995). One type of proposed mechanism is Langmuir-Hinshelwood type adsorptive mechanism, where CO and H_2O adsorb on the catalyst surface. Dissociated water forms reactive hydroxyl groups and these hydroxyl groups react with adsorbed CO to produce a formate intermediate, which is then decomposes into adsorbed hydrogen and CO_2. The steps of the adsorptive mechanism are described as follows, where * represents active metal sites (Ladebeck and Wagner, 2003; Choi and Stenger, 2003):

$$CO + * \leftrightarrow CO^* \quad (2.7)$$

$$H_2O + 2^* \leftrightarrow H^* + OH^* \quad (2.8)$$

$$OH^* + CO^* \leftrightarrow HCOO^* + * \quad (2.9)$$

$$HCOO^* + * \leftrightarrow CO_2^* + H^* \quad (2.10)$$

$$CO_2^* \leftrightarrow CO_2 + * \quad (2.11)$$

$$2H^* \leftrightarrow H_2 + 2^* \quad (2.12)$$

Numerous studies have been conducted to prove the mechanism by detecting formate species through isotopic labeling, chemical trapping experiments and FTIR analyses (Choi and Stenger, 2003). Shido and Iwasawa (1993) found that for the adsorptive mechanism, the decomposition of the formate was the rate determining step and they also indicated that increasing water partial pressure in the feed increased the rate of formate decomposition and the activation energy decreased.

The other approach, regenerative or redox mechanism, which is based on Rideal-Eley type mechanism, is shown in Equations 2.13 and 2.14, where “Red” refers reduced sites and “Ox” refers oxidized sites. This mechanism basically consists of two cycling steps and it requires a redox species on the catalyst. At this cycle water adsorbs on the reduced surface, produces H_2 by dissociation and oxidizes the surface. Subsequently CO re-reduced the oxidized surface and forms CO_2 (Choi and Stenger, 2003; Kolb *et al.*, 2005). In another

description of the bi-functional mechanism, it is explained that CO adsorbs on the active metal or metal oxide and oxidized by the support, while water refills the support's oxygen vacancy (Ladebeck and Wagner, 2003).

$$H_2O + Red \rightarrow H_2 + Ox \quad (2.13)$$

$$CO + Ox \rightarrow CO_2 + Red \quad (2.14)$$

Ceria is a widely used redox material. Because they are not easily oxidized by the water, precious metals like Pt, Pd and Rh are not effective WGS catalysts. However introducing ceria to the catalyst significantly increases the reaction rate. When regenerative mechanism is considered it is seen that Ce_2O_3 is easily oxidized by H_2O and releases H_2, as CO is oxidized by CeO_2 and convert into CO_2. This mechanism can be presented as below for ceria catalysts, where σ indicates adsorption sites of the metal (Bunluesin *et al*., 1998):

$$CO + \sigma \rightarrow CO_{ad} \quad (2.15)$$

$$H_2O + Ce_2O_3 \rightarrow H_2 + 2CeO_2 \quad (2.16)$$

$$CO_{ad} + 2CeO_2 \rightarrow CO_2 + Ce_2O_3 + \sigma \quad (2.17)$$

Gorte and Zhao (2005) investigated the WGS reaction mechanism over ceria based Pd and Pt catalysts at $H_2O/CO=1$ and they expressed that the study confirmed the reaction proceeds by the redox mechanism. They reported that the redox mechanism steps were detected by pulse-reactor measurements and this mechanism fitted accurately to observed rate expressions. Additionally, it was indicated that the reaction rate increased with increasing temperature and it reduced the possibility of the presence of adsorptive mechanism, since formates have limited thermal stability so high reaction rates should had been observed at low temperatures.

Li *et al*. (2000) studied Cu and Ni loaded ceria catalysts' kinetic behavior in the temperature range 175-300 °C and their study also revealed that the redox model was acceptable for WGS. They proposed the following rate expression (Equation 2.18) for ceria mediated redox process and it was reported that at low P_{CO}/P_{H_2O} the reaction was first order in CO and zero order in H_2O, and at high P_{CO}/P_{H_2O} values the opposite case was valid.

$$\text{Rate}=\frac{k_1 k_2\, P_{CO} P_{H_2O}}{k_1 P_{CO} + k_2 P_{H_2O}} \tag{2.18}$$

The kinetic study of Koryabkina *et al.* (2003) on Cu-based catalysts under real reformer conditions supports surface redox mechanism too and the reduction of surface oxygen by adsorbed CO was considered as a rate determining step. For industrial CuZnAl catalyst reaction orders for CO and H_2O were found to be 0.8 and for CO and H_2 -0.9. The rate per unit of Cu surface area was measured almost same for all the catalysts tested, therefore it was indicated that the reaction occurred only on Cu surface and addition of ceria or ZnO to the catalyst did not affect rate.

Another study of mechanism for WGS was conducted by Hilaire *et al*. (2001) over ceria supported Pd catalyst with 1wt.% metal loading and redox model was supported. At operating conditions the reaction orders were found to be zero and one-half for CO and H_2O, respectively. The zero order dependence for CO was attributed to saturation of Pd surface with CO, hence the rate was not influenced by the changes in CO pressure. The half order dependence for H_2O showed that the rate was partially limited by re-oxidation of ceria. The rates for CO_2 and H_2 were found to be inverse-half order and inverse-order, respectively and the rate expression for Pd/ceria catalyst was described as follows (Ladebeck and Wagner, 2003):

$$r_{Pd}=\frac{k_{Pd}\left(P_{H_2O}^{0.5}\right)}{\left(P_{CO_2}^{0.5}\, P_{H_2}\right)}(1\text{-}\beta) \tag{2.19}$$

where β was defined by Equation 2.20.

$$\beta=\frac{\left(P_{CO_2} P_{H_2}\right)}{\left(P_{CO}\, P_{H_2O}\right)}\frac{1}{K_{eq}} \tag{2.20}$$

The FTIR measurements detected “carbonate” formation on ceria during WGS and reduction of Pd/ceria by pure CO. These findings supported redox mechanism since carbonate decomposed when exposed to H_2O. The authors suggested that the carbonate

was not take place in WGS mechanism because as the ceria was oxidized by water it made carbonate unstable and removed it (Hilaire *et al*., 2001).

On the contrary, Jacobs *et al.* (2003) performed DRIFT studies for WGS reaction over Pt/CeO_2 catalyst at high H_2O/CO ratio, where the rate dependency of CO is first order. From DRIFT analyses, in contrast to previous studies explained above, the formation of formate was detected especially at low temperatures. As the temperature increased, the coverage of surface formates was limited by WGS and hence the CO conversion was higher. They also noted that decreasing the size of the ceria particles and high noble metal loading and dispersion limited the rate of the formation of surface formates too which resulted in higher catalyst performance.

2.5. Microchannel Reactors

The idea of microchannel process technology had been arised in 1960s for heat exchanger applications and reactions were integrated to this process in 1990s. With this technology heat exchange, mixing, chemical reactions and chemical separation can take place in a single unit; hence traditional reactor systems may be replaced by more flexible, faster and cost effective units (Tonkovich *et al*., 2005; Mills *et al*., 2007). The benefits of the microchannel technology are related with the small channel diameters in which high heat and mass transfer rates can be achieved under laminar flow conditions (Tonkovich *et al*., 2004).

Microchannel reactors consist of parallel, identical channels with diameters between 10 to several hundred micrometers that result in high surface to volume ratio in the range of 10000-50000 m^2/m^3, which is generally about 100 m^2/m^3 for conventional vessels. High surface to volume ratio improves the heat transfer rate between the reactor wall and the reaction zone, thus more efficient use of catalysts can be achieved, especially for highly exothermic or endothermic reactions, and prevent the hot spot formation (Kiwi-Minsker and Renken, 2005). As compared to traditional large scale reactors, short diffusional rates increase the conversion rates in microreactors significantly, as the amount of catalyst needed is decreased. Additionally narrow residence time distribution enhances the selectivity of desired product (Ehrfeld *et al*., 2000).

As mentioned before, due to the thermodynamic and kinetic limitations conventionally WGS reaction consists of two separate fixed bed reactors with intermediate cooling section which operate at different temperature ranges. In order to integrate WGS reaction into mobile fuel cell applications and on-board hydrogen production the size of the reactor must be minimized. At this point microchannel reactors play an important role. As microchannel reactor is integrated with heat exchanger, the system can be maintained at optimum temperature along the reactor, thus these two step process can be replaced by a single unit and the size of the system is reduced significantly (Baier and Kolb, 2007).

The important point that should be taken into consideration for microchannel reactors is the type of the catalyst used. Packing of catalyst powders or coated pellets used for traditional fixed-bed reactors irregularly would remove the benefits of the microreactors and formation of hot spots and pressure drop could be observed due to the non-uniform flow profile. In order to avoid these drawbacks microscale catalyst powders are applied and they are coated on microstructured surfaces by several techniques such as wet impregnation and sol-gel process (Ehrfeld *et al*., 2000).

Germani *et al*. (2005) tested the activity of platinum/ceria/alumina catalyst for WGS reaction in a microchannel reactor. Stainless steel micro-structured plates were coated by sol-gel method and strongly adhesive and stable catalyst layers were obtained. The comparison of CO conversions for the powder and the coated catalyst showed that powder catalyst sample exhibited much lower activity than the coated one and at temperatures above 260 °C this difference became larger. The diffusion limitations inside the powder pellets were thought to be the reason of this behavior. At this work it was also noted that changing the amount of ceria content in the catalyst did not affect the catalyst activity to a great extent.

Goerke and coworkers (2004) studied WGS reaction in microchannels coated with Rh/ZrO_2 and Au/CeO_2 catalysts. It was observed that, even it was sufficient for the reaction tests, adhesion of CeO_2 supported catalysts is not as good as the ZrO_2 based catalyst. By SEM analyses cracks were detected on CeO_2 based catalysts and heterogeneous distribution of catalyst over stainless steel foil was observed. In contrast to CeO_2, ZrO_2 supported catalyst was distributed homogeneously and no significant cracks

were seen. In reaction tests Rh/ZrO_2 showed the highest activity at 310 °C with 96% CO conversion, while Au/CeO_2 catalyst reached maximum activity at 370 °C with only 3.7% conversion.

The comparative study of platinum group metal catalysts supported on wash coated alumina was conducted by Kolb and colleagues (2005). The effect of addition of Rh, Ru and Pd metals to Pt/ceria/alumina catalyst with 4 wt.% Pt content was investigated and it was concluded that among these catalysts Pt/ceria/alumina was the most promising catalyst for LTS and HTS reactions, while Pt/Pd/ceria/alumina showed the lowest activity in either case. The samples containing Ru and Rh exhibited significant selectivity towards methanation reaction under LTS and HTS conditions. Similar findings to Germani *et al*. (2005) have been reported in terms of the effect of catalyst's ceria content. It was seen that increasing ceria content from 12wt.% to 24wt.% had no significant impact on the catalyst activity.

3. EXPERIMENTAL WORK

3.1. Materials

3.1.1. Chemicals

All the chemicals used for catalyst preparation are presented in Table 3.1.

Table 3.1. Chemicals used for catalyst synthesis.

Chemicals	Specification	Source	Molecular weight
Palladium(II) nitrate hydrate	$Pd(NO_3)_2.xH_2O$	Sigma-Aldrich	230.43
Cerium(III) nitrate hexahydrate	$Ce(NO_3)_3.6H_2O$ (99.99%)	Sigma Aldrich	434.22
Gamma alumina	γ-Al_2O_3	Alfa-Aesar	101.96
Gamma alumina (3 μm)	γ-Al_2O_3 80-120 m^2/g	Alfa-Aesar	101.96

3.1.2. Gases and Liquids

The gases N_2, CO, H_2, CO_2, Ar, He and dry air used in experimental studies (Table 3.3) were supplied by Linde. The deionized water is obtained by Zeneer Water Purification System.

Table 3.2. Specifications and the applications of liquids used in experiments.

Liquid	Specification	Applications
Water	Deionized water Conductivity less than 0.1 $\mu S.cm^{-1}$	Catalyst synthesis, Reactant

Table 3.3. Specifications and applications of the gases used.

Gas	Specification	Application
Argon	99.995% (Linde)	GC carrier gas
Helium	99.99% (Linde)	GC carrier gas
Nitrogen	99.99% (Linde)	GC calibration, inert
Carbon monoxide	99.999% (Linde)	GC calibration, reactant
Hydrogen	99.99% (Linde)	GC calibration, reducing agent
Carbon dioxide	99.99% (Linde)	GC calibration
Methane	99.70% (Linde)	GC calibration
Dry air	78.4%N_2+21.5% O_2 (Linde)	GC calibration

3.2. Experimental Systems

The experimental system used in this research mainly consists of four groups.

- Catalyst Preparation System: The setup used for preparing all the catalysts used in this study by incipient-to-wetness impregnation method.
- Catalyst Characterization System: Scanning Electron Microscopy (SEM) integrated with Energy Dispersive X-ray Spectroscopy (EDX) to analyze the structural properties of the catalysts.
- Catalytic Reaction System: The system used for catalytic activity tests, consisting of mass flow controllers for inlet gases, HPLC pump for water feed, temperature controlled heated connecting lines, reaction chamber controlled by a programmable temperature controller and a fixed-bed reactor.
- Product Analysis System: Two online gas chromatographs are used for analyzing the composition of the reactant and product gases.

3.2.1. Catalyst Preparation System

Pd/CeO_2 and $Pd\text{-}CeO_2/Al_2O_3$ catalysts are prepared by incipient to wetness impregnation method illustrated by Figure 3.1. The system includes Retsch UR1 ultrasonic

mixer, a vacuum pump, a vacuum flask and a Masterflex computerized-drive peristaltic pump which is used for impregnation of the solution to the support.

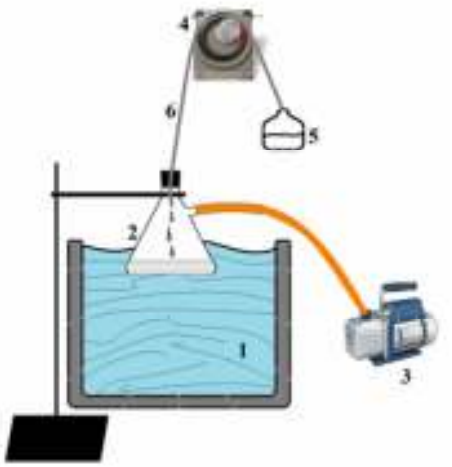

Figure 3.1. The Impregnation System: 1. Ultrasonic Mixer 2. Vacuum Flask 3.Vacuum Pump 4. Peristaltic Pump 5.Aqueous Catalyst Solution 6. Silicon Tubing (Karakaya, 2012).

3.2.2. Catalyst Characterization System

The structural analyses of the catalyst samples were carried out at Boğaziçi University Advanced Technologies R&D Center through Backscattering Electron-Scanning Electron Microscopy (BSE-SEM) and Energy Dispersive X-ray Analyses (EDX) using a Philips XL30 ESEM-FEG system.

3.2.3. Catalytic Reaction System

The Water Gas Shift reaction system was designed and constructed at CATREL, Department of Chemical Engineering. The system is mainly composed of three sections (Figure 3.2):

- Feed section
- Reaction section
- Product analysis section.

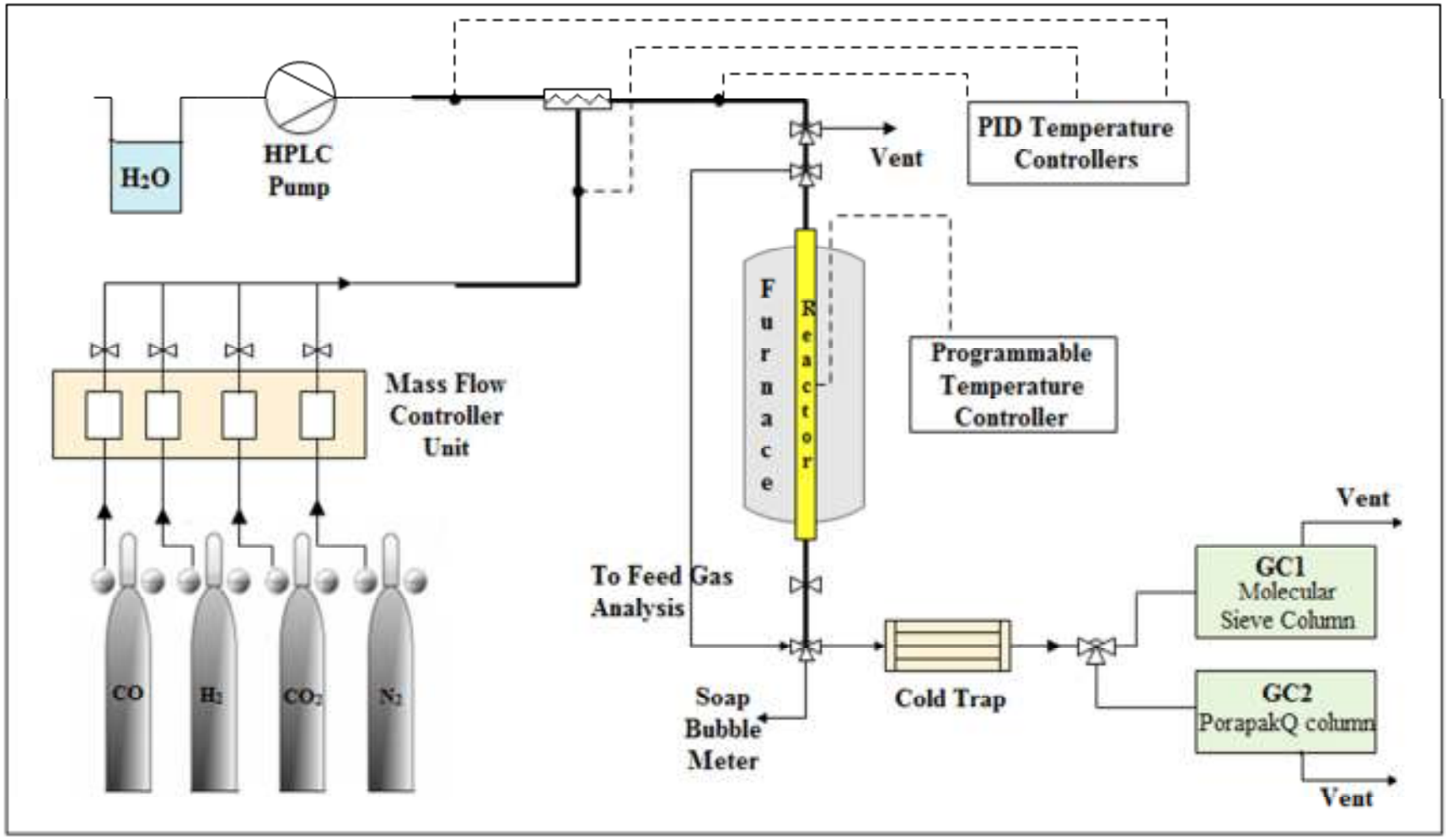

Figure 3.2. Schematic Diagram of the Reaction System.

The feed section includes mass flow controllers, 1/4", 1/8" and 1/16" stainless steel and brass tubes and fittings for feeding the reactants to the system. The research grades of pure N_2, CO, H_2, CO_2 and CH_4 gases in pressurized cylinders are passed through the gas flow regulators to the system. The flow rates of the gases are controlled by Brooks 5850E mass flow controllers and the set point values are adjusted by Brooks 0154 control panel. The mass flow controllers were calibrated for each gas and the calibration curves were given in Appendix A. The 1/4" stainless steel tubes were used for inlet and the outlet of the mass flow controllers till the mixing part and on-off valves were placed in front the mass flow controllers in order to prevent back-pressure fluctuations. In order to provide homogeneous gas mixture, the gases are passed through mixing zone before meeting with water, which is kept at 125 °C by heating tape and PID temperature controller with K-type thermocouple.

The deionized water is introduced to the system at a constant flow rates by Agilent 1200 Isocratic HPLC pump. Liquid water is passed through 1/16" stainless steel tube and the tube is kept at 125 °C by heating tape and a temperature controller, to feed the water in the form of steam before mixing with other gaseous reactants.

The mixing zone of steam and other gaseous reactants consists of 1/16" stainless steel tube and the diameter of the lines is gradually increased to 1/8" and 1/4". During the mixing period in order to reach a steady state flow, the gas stream is sent to the vent line using a three-way valve for at least 30 min. The feed gases could be also sent to the by-pass line by second three-way valve, so that the feed composition could be analyzed by gas chromatographs before the reaction. After feed analyses the feed stream is sent to the reaction zone which consists of 1/4" stainless steel tubes and furnace controlled by Shimaden FP23 programmable temperature controller. For conventional fixed bed experiments 1/4" stainless steel reactor is used, while 2.0 cm ID x 78 cm quartz reactor is used for microreaction tests. The catalyst bed is located at the center of the furnace and the K-type thermocouple is placed near the center of the catalyst bed around the reactor to control the reaction temperature. The system was covered by glass wool insulations to prevent heat loss.

The third three-way valve was placed at the exit of the reactor which shifts the flow between a soap bubble meter, which is necessary to measure and control of the gas flow rate at the exit of the reactor, and a line that is connected to gas chromatographs. Since GC column materials are highly sensitive to the liquid water, the exit stream of the reactor is passed through an ice cold trap in order to condense the remaining water vapor before entering the GC unit. The detailed properties of the gas chromatographs and the description of the gas analysis are given in the following section.

3.2.4. Product Analysis System

The feed and the product stream compositions are quantified by two online gas chromatographs on a dry basis. HP Agilent 6890N gas chromatography (GC1), equipped with Molecular Sieve 5A column and TCD detector is used for the measurements of carbon monoxide, hydrogen and nitrogen; while HP Agilent 6850N (GC2) equipped with Porapak Q column and TCD detector is used for carbon dioxide and methane measurements. The stream coming from the cold trap is sent continuously to the GC1 and after gas sampling, the flow is diverted to GC2 by three-way valve. Before reaction tests optimized GC parameters were determined as listed in Table 3.4.

Table 3.4. GC conditions for reactant and product analyses.

GC Parameter	**HP Agilent 6890N**	**HP Agilent 6850N**
Detector type	Thermal conductivity	Thermal conductivity
Column oven temperature	40 °C	40 °C
Injector temperature	80 °C	110 °C
Detector temperature	150 °C	150 °C
Carrier gas	Argon	Helium
Carrier gas flow rate	25 $ml.min^{-1}$	20 $ml.min^{-1}$
Column packing material	Molecular Sieve 5A (60-80 mesh)	Porapak Q (80-100 mesh)
Column tubing material	Stainless steel	Stainless steel
Column ID & length	1/8" OD x 2 m	1/8" OD x 3 m
Sampling loop	1 ml	1 ml

Before the experiments the calibrations of both gas chromatographs were done by injecting known volumes of the species separately to the columns under the optimum conditions given in Table 3.4. In the chromatograph each gas forms a peak at specific retention times and the area under these peaks are calculated by integrator software. Micromole versus peak area graphs was plotted and the calibration curves were constructed as presented in Appendix B.

3.3. Catalyst Preparation and Pretreatment

In this research the catalytic activity of Pd/CeO_2, $Pd\text{-}CeO_2/Al_2O_3$ and Pd/TiO_2 catalysts for water gas shift reaction were tested. The catalysts are prepared by incipient to wetness impregnation method. Catalyst preparation procedure includes support preparation, synthesis of active catalysts and pretreatment steps.

3.3.1. Preparation of Pd/CeO_2 Catalyst

The 1.5wt.%Pd/CeO_2 catalyst is prepared by incipient to wetness impregnation method by using the system illustrated in Figure 3.1. The catalyst synthesis process mainly consists of four steps:

- Support preparation
- Contacting the support with the precursor solution
- Drying
- Calcination

At first step ceria support is prepared by thermal decomposition of cerium nitrate ($Ce(NO_3)_3.6H_2O$), taking into consideration of the study of Zheng *et al*. (2005). Cerium nitrate salt is kept at 600 °C for 4 hours in muffle furnace. Then the obtained powder is crushed and sieved into 45-60 mesh (250-354μm) size for packed-bed reactor experiments. This catalyst was also studied at microstructured reactor experiments. For packed microchannel tests containing particulate catalyst, 60-80 mesh particle size ceria is used for catalyst synthesis, while for wall coated microchannel tests ceria with particle size above 100 mesh is utilized.

Before the impregnation, prepared support is dried in vacuum oven at 105 °C for 1 hour and then it is put in a vacuum flask and mixed with ultrasonic mixer for 30 min under vacuum. A calculated amount of Pd precursor is dissolved in 0.9 ml deionized water per gram of ceria support. This aqueous solution is impregnated over the support via peristaltic pump at a constant flow rate of 0.5 $ml.min^{-1}$. The slurry is mixed ultrasonically during impregnation to obtain uniform distribution of the active metal on the support. After impregnation the mixing continues for 90 min under vacuum. The resulting slurry is dried at 115 °C overnight and then calcined at 400ºC in a muffle furnace for 2 hours.

3.3.2. Preparation of Pd-CeO_2/Al_2O_3 Catalyst

The Pd-CeO_2/Al_2O_3 catalyst is prepared by sequential impregnation method according to the composition of 1.5wt.%Pd−20wt%CeO_2/ γ-Al_2O_3.

Commercial γ-Al_2O_3 is used as a support material for this catalyst. Before impregnation γ-Al_2O_3 is crushed and sieved into 45-60 mesh size (250-354 μm) and dried in vacuum oven at 105 °C for 1 hour. A definite amount of γ-Al_2O_3 is put in a vacuum flask kept under vacuum and mixed with ultrasonic mixer for 30 min.

At first impregnation step cerium nitrate solution is fed to the vacuum flask. A calculated amount of $Ce(NO_3)_3.6H_2O$ salt was dissolved in 1.0 ml of deionized water per gram of catalyst and impregnated over γ-Al_2O_3 support and mixed ultrasonically for 90 min. The resulting slurry is dried at 115 °C overnight (16 hours) and calcined at 300 °C in a muffle furnace for 2 hours.

In the second step of the impregnation, ceria impregnated alumina support is put in vacuum flask again and mixed with ultrasonic mixer for 30 min under vacuum. A calculated amount of $Pd(NO_3)_2.xH_2O$ is dissolved in 1.1 ml of deionized water per gram of catalyst. The Pd solution is fed to the vacuum flask with same procedure described above and mixed for 90 min. The resulting Pd-CeO_2/Al_2O_3 catalyst is dried at 115 °C overnight (16 hours) and calcined at 300 °C in a muffle furnace for 2 hours.

3.3.3. Preparation of Pd/TiO_2 Catalyst

The 1.5wt.%Pd/TiO_2 catalyst is prepared by incipient to wetness impregnation method according to the study of Aktürk (2011).

The TiO_2 support is first sieved into 45-60 mesh size (250-354 μm) and calcined at 500 °C for 4 hours in a muffle furnace. The prepared support is put in a vacuum flask and mixed for 30 min. The calculated amount of Pd precursor is dissolved in 0.8 ml deionized water per gram of support and this aqueous solution is impregnated over TiO_2 by the same procedure described above. After impregnation the resulting slurry is dried at 115 °C overnight and calcined at 500 °C for 4 hours.

3.3.4. Catalyst Coating on Microchannel Plates

The activity test of 1.5wt.%Pd/CeO_2 catalyst was also conducted at microstructured reactor. The microstructured reactor basically consists of 310-grade stainless steel H-shaped cylindrical housing with diameter D=18.6 mm, and length L= 30 mm and two FeCrAlY plates with dimensions of 2 mm x 5 mm x 20 mm, which are inserted into steel housing.

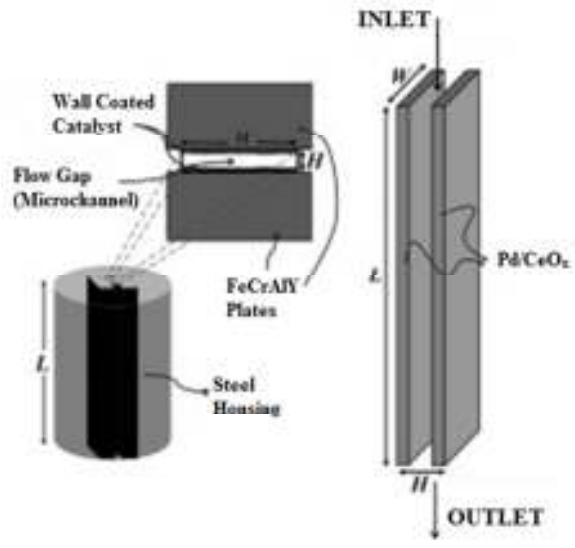

Figure 3.3. H-type Steel Housing including Two Coated Plates and Catalytic Microchannel (Şimşek *et al*., 2013).

The catalyst coated on microstructured plates is prepared by incipient to wetness impregnation method described as above and ceria with less than 100 mesh particle size is used as a catalyst support. Catalyst coating step includes several chemical and mechanical treatment procedures. First of all the housing and the plates are needed to be cleaned properly and dried at 110 °C for 2 hours. In the next step, to enhance the adhesion of the coated plates, they are calcined at 900 °C for 3 hours in a muffle furnace; hence native alumina layer is formed on the plates. After the housing and the plates are ready for the coating operation, the previously calcined Pd/ceria catalyst powder is wetted by deionized water very lightly and the resulting slurries are blade coated on to 5 mm x 20 mm plates. In this research each two plates are coated by net 10 mg powder catalyst. The coated plates are dried at 115 °C overnight and they are calcined at the reaction temperature for 3 hours. In the last step the coated plates are inserted into cylindrical housing. The possible displacement of the plates is prevented by inserting 10 mm height ceramic wool at the bottom of the housing. At the end of this process one rectangular microchannel with dimensions 0.75 mm (height) x 4 mm (width) x 20 mm (length) is created.

3.3.5. Pretreatment

During the calcination step active metals of the catalysts transform into oxidized state, therefore active metals must be reduced into metallic state in order to enhance the catalytic activity. All of the Pd based catalysts are reduced before the water gas shift reaction under 50 $ml.min^{-1}$ H_2 flow for 3 hours at reaction temperatures and kept under N_2 until the reaction test is started.

3.4. Reaction Tests

3.4.1. Blank Tests

In order to ensure that the material of construction (stainless steel, quartz and FeCrAlY) and glass wool are inert towards the reactants, blank tests are conducted under reaction conditions. The effluent stream is analyzed by GCs and no indications of water gas shift reaction are observed.

3.4.2. WGS in Conventional Packed Bed Reactor

The water gas shift reaction is investigated in conventional 1/4" stainless steel reactor system over Pd/CeO_2, $Pd\text{-}CeO_2/Al_2O_3$ and Pd/TiO_2 catalysts. The catalyst is packed into the center of the reactor and supported underneath by glass wool with 1 cm height. The temperature of the reaction zone is measured by K-type thermocouple which is placed near the catalyst bed outside the reactor wall and connected to programmable temperature controller.

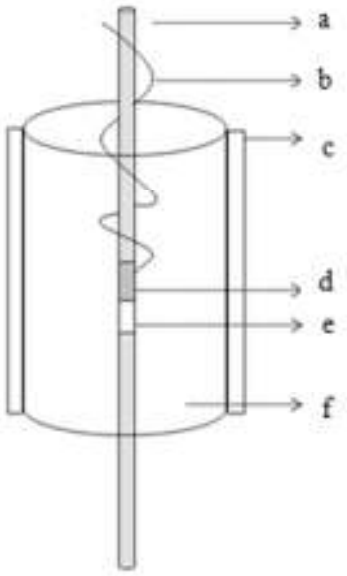

Figure 3.4. Schematic Diagram of the Conventional Packed Bed Reactor and Furnace System: A. Reactor B. Thermocouple C. Ceramic Wool İnsulation D. Catalyst E. Glass Wool f. Furnace.

The reaction conditions used for Pd based catalysts are summarized in Table 3.4. The type of catalyst, reaction temperature, H_2O/CO ratio and catalyst weight are changed in order to determine the effect of these parameters on the catalyst activity. The feed composition consists of CO and H_2O, balanced with 30 $ml.min^{-1}$ N_2. The total flow rate is kept constant at 70 $ml.min^{-1}$ for all the experiments. The list of the experiments over Pd based catalysts is given in Table 3.5.

Table 3.5. Reaction conditions for catalytic activity tests.

Parameter	Value
Catalyst Particle Size (mesh size)	45-60, 60-80
Catalyst Amount (mg)	20, 100
Reduction Temperature (°C)	250, 300, 325
Reaction Temperature (°C)	250, 300, 325
Reaction Total Flow rate (ml.min^{-1})	70
W/F Ratio (mg.min.ml^{-1})	0.29, 1.43

Table 3.6. List of experiments on Pd based catalysts in conventional packed bed reactor.

#	Catalyst	Temp. (°C)	W_{cat} (mg)	S/C	CO (ml.min^{-1})	H_2O (ml.min^{-1})	Particle mesh size
1	1.5%Pd/CeO_2	250	100	1	20	20	45-60
2	1.5%Pd/CeO_2	250	100	1.67	15	25	45-60
3	1.5%Pd/CeO_2	250	100	3	10	30	45-60
4	1.5%Pd/CeO_2	250	100	5	6.7	33.3	45-60
5	1.5%Pd/CeO_2	300	100	1	20	20	45-60
6	1.5%Pd/CeO_2	300	100	1.67	15	25	45-60
7	1.5%Pd/CeO_2	300	100	3	10	30	45-60
8	1.5%Pd/CeO_2	300	100	5	6.7	33.3	45-60
9	1.5%Pd/CeO_2	325	100	1	20	20	45-60
10	1.5%Pd/CeO_2	325	100	1.67	15	25	45-60
11	1.5%Pd/CeO_2	325	100	3	10	30	45-60
12	1.5%Pd/CeO_2	325	100	5	6.7	33.3	45-60
13	1.5%Pd-20%CeO_2/Al_2O_3	300	100	1	20	20	45-60
14	1.5%Pd-20%CeO_2/Al_2O_3	300	100	1.67	15	25	45-60
15	1.5%Pd-20%CeO_2/Al_2O_3	300	100	3	10	30	45-60
16	1.5%Pd-20%CeO_2/Al_2O_3	300	100	5	6.7	33.3	45-60
17	1.5%Pd/TiO_2	300	100	1	20	20	45-60
18	1.5%Pd/TiO_2	300	100	3	10	30	45-60

3.4.3. WGS in Microchannel Reactor

Microchannel experiments are conducted by using quartz tube having inner diameter ID=20 mm, H-shaped steel housing and two FeCrAlY plates. The housing, including FeCrAlY plates, is inserted in the middle of the quartz tube and supported underneath by hollow ring as shown in Figure 3.5b; thus the housing is fixed in desired position and bypass through the annulus between the housing and the quartz tube is prevented. Same as conventional packed bed reactor system, the temperature of the reaction zone is measured by K-type thermocouple located inside the tube furnace and contacts with the central point of the quartz tube.

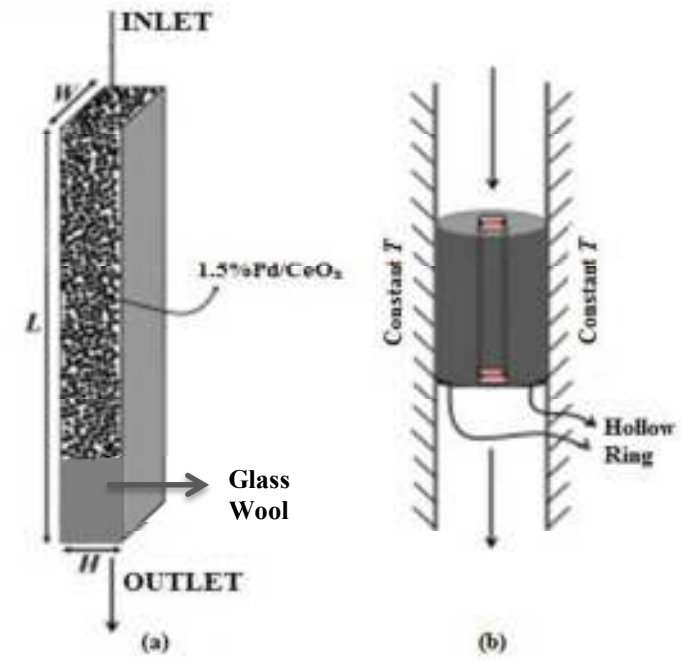

Figure 3.5. Packed Microchannel Configuration a. Packed Microchannel Reactor b. Location of the Metallic Block inside the Quartz Tube (Şimşek *et al*., 2013).

The WGS reaction is tested over particulate and wall-coated 1.5wt.%Pd/CeO_2 catalysts. The catalyst tested for wall-coated system is prepared by using CeO_2 support with particle size above 100 mesh and the coated plates are prepared according to the procedure described at Section 3.3.4. The wall-coated microchannel reactor experiments are conducted at 325 °C, S/C=5. However, during WGS reaction it is observed that the adhesion between the FeCrAlY plate and ceria supported catalyst is not sufficient enough

to endure the reaction conditions. Therefore microreaction studies are focused on packed microchannel reactor systems.

1.5wt.%Pd/CeO_2 catalyst, which contains CeO_2 support with 60-80 mesh size, is used for packed microchannel reaction experiments. In this configuration two uncoated plates are inserted into steel housing and a rectangular microchannel with dimensions 0.75 mm (height) x 4 mm (width) x 20 mm (length) is created. As shown in Figure 3.5a the channel is filled with 20 mg particulate catalyst and supported underneath by glass wool to fix the catalyst bed. The list of experiments performed over this structure is presented in Table 3.6. At all the experiments the total flow rate is fixed at 70 ml.min^{-1}. The feed stream consists of CO, H_2O and N_2 with 30 ml.min^{-1} flow rate.

Table 3.7. List of experiments on Pd based catalyst in packed microchannel reactor.

#	Catalyst	Temp. (°C)	W_{cat} (mg)	S/C	CO (ml.min^{-1})	H_2O (ml.min^{-1})	Particle mesh size
19	1.5%Pd/CeO_2	300	20	1	20	20	60-80
20	1.5%Pd/CeO_2	300	20	1.67	15	25	60-80
21	1.5%Pd/CeO_2	300	20	3	10	30	60-80
22	1.5%Pd/CeO_2	300	20	5	6.7	33.3	60-80
23	1.5%Pd/CeO_2	325	20	1	20	20	60-80
24	1.5%Pd/CeO_2	325	20	1.67	15	25	60-80
25	1.5%Pd/CeO_2	325	20	3	10	30	60-80
26	1.5%Pd/CeO_2	325	20	5	6.7	33.3	60-80

The comparisons of the results obtained from this study is done in terms of CO conversions, which calculated by taking the ratio of consumed CO to the inlet CO (Equation 3.1).

$$X_{CO}=100\times\frac{F_{CO}^{in}-F_{CO}^{out}}{F_{CO}^{in}} \tag{3.1}$$

4. RESULTS AND DISCUSSION

The results of this study are reported in two sections. In the first section the performances of Pd/CeO_2, $Pd\text{-}CeO_2/Al_2O_3$ and Pd/TiO_2 catalysts on WGS in stainless steel packed bed reactor are compared at various reaction temperatures and steam to carbon (S/C) ratios. These comparisons are conducted in terms of CO conversions, which are calculated by Equation 3.1. SEM analysis results of Pd/CeO_2 and $Pd\text{-}CeO_2/Al_2O_3$ catalysts are also reported to point out the changes on catalyst surface and active metallic sites after they expose to reaction.

The second section includes the comparison of the Pd/CeO_2 activity for WGS in conventional fixed bed and packed microchannel reactor configurations. The effect of temperature and S/C on WGS is also presented for microchannel reactor structure. The comparisons are done in terms of productivity, which can be defined as % CO conversion per unit amount of catalyst (Equation 4.1).

$$\text{Productivity} = \frac{X_{CO}}{\text{Catalyst weight (mg)}} \tag{4.1}$$

The experimental error is found to be less than 8% throughout this study.

4.1. WGS in Conventional Packed Bed Reactor

The first section of this study can be handled in two parts. In the first part, detailed parametric experiments were performed over $1.5\%Pd/CeO_2$ catalyst in 1/4 inch stainless steel reactor. This reactor involves 100 mg of catalyst with 45-60 mesh size. In order to determine the effect of temperature and S/C, these experiments were conducted at 250, 300 and 325 °C at atmospheric pressure with S/C ratios of 1, 1.67, 3 and 5. The total flow and N_2 flow rates were kept constant at 70 $ml.min^{-1}$ and 30 $ml.min^{-1}$, respectively and the H_2O and CO compositions were arranged as presented in, Table 3.6. The calculated CO conversions are shown in Figure 4.1.

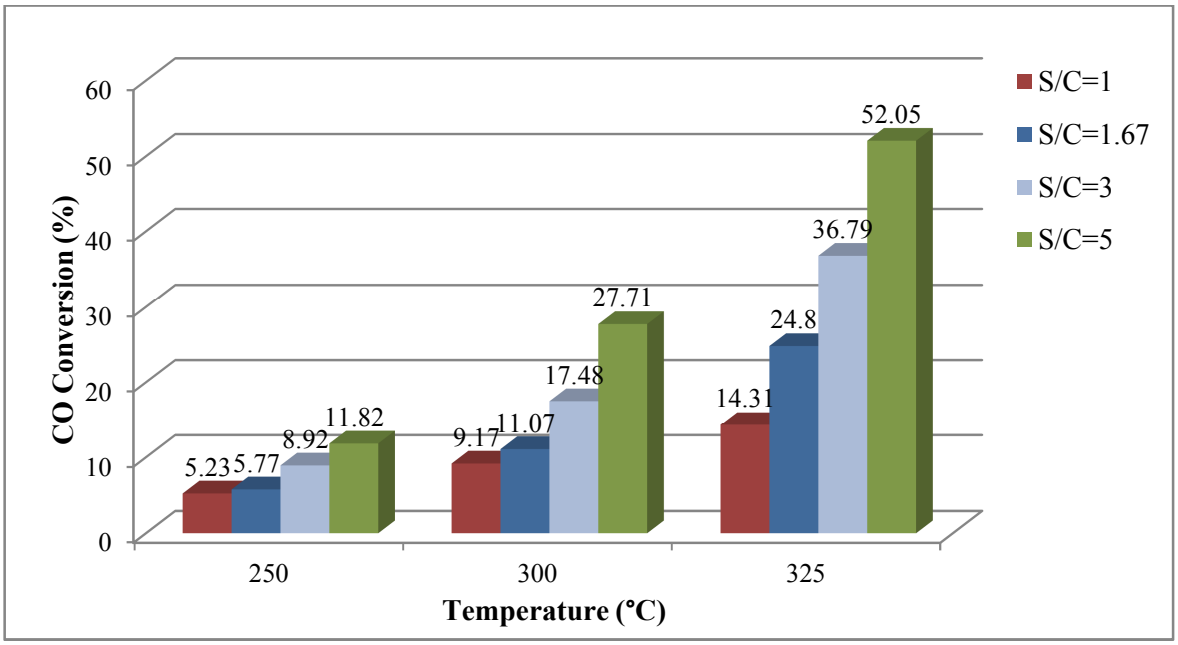

Figure 4.1. Effect of Temperature and S/C on CO Conversion over 1.5%Pd/CeO_2 Catalyst.

As a result of these experiments, as shown in Figure 4.1, improvement in CO conversion is observed with increasing temperature. While the maximum CO conversion is only 12% at 250 °C and S/C=5, this value reaches 28% and 52% at 300 and 325 °C, respectively. It can be concluded that in the 250-325 °C range, WGS reaction over Pd/CeO_2 catalyst is controlled by chemical kinetics (Chen *et al*., 2008). In the literature it is reported that the rate of WGS is proportional to steam partial pressure (Choi and Stenger, 2003). The experimental results align with this fact. Increasing S/C value from 1 to 5 stimulates WGS and the differences in CO conversion values at different S/C ratios become wider at higher temperatures, which supports the fact that the reaction is kinetically controlled.

Figure 4.2 and 4.3 present changes in CO % in product stream during reaction tests at 300 °C and 325 °C. In all experiments sharp decline of CO content was detected at first 75 minutes and steady state was reached after approximately 120 minutes. CO conversion values and product compositions were calculated by taking the average of data obtained after this time.

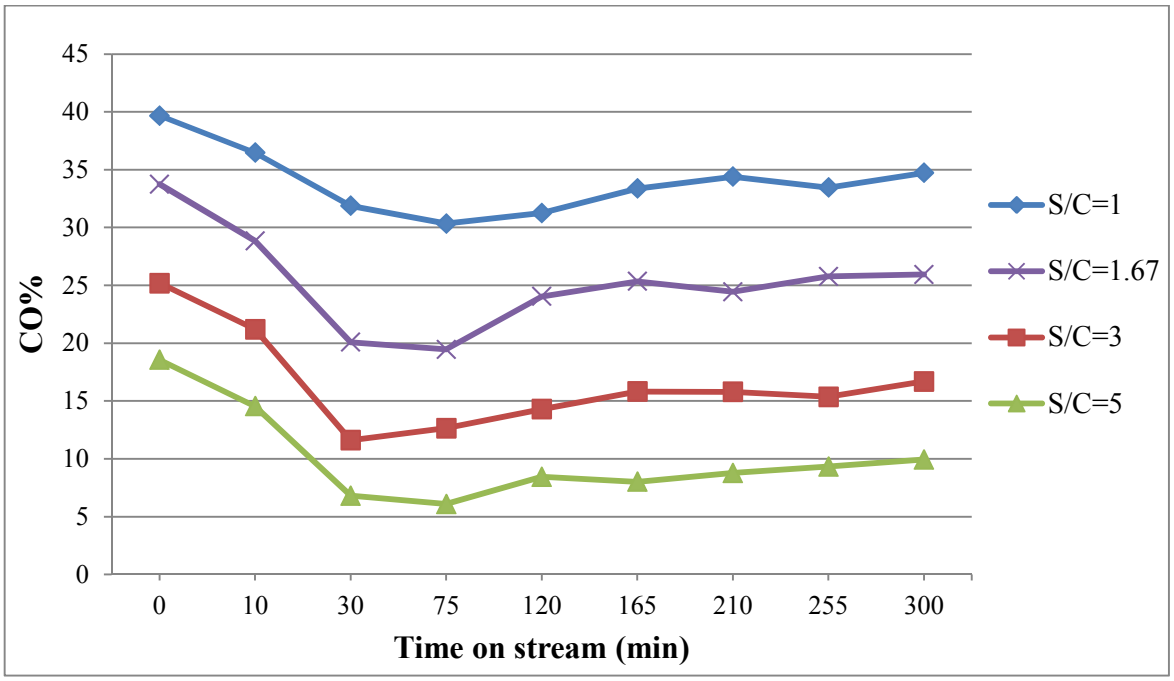

Figure 4.2. CO Content in the Product Stream during Reaction over Pd/CeO_2 at 325 °C.

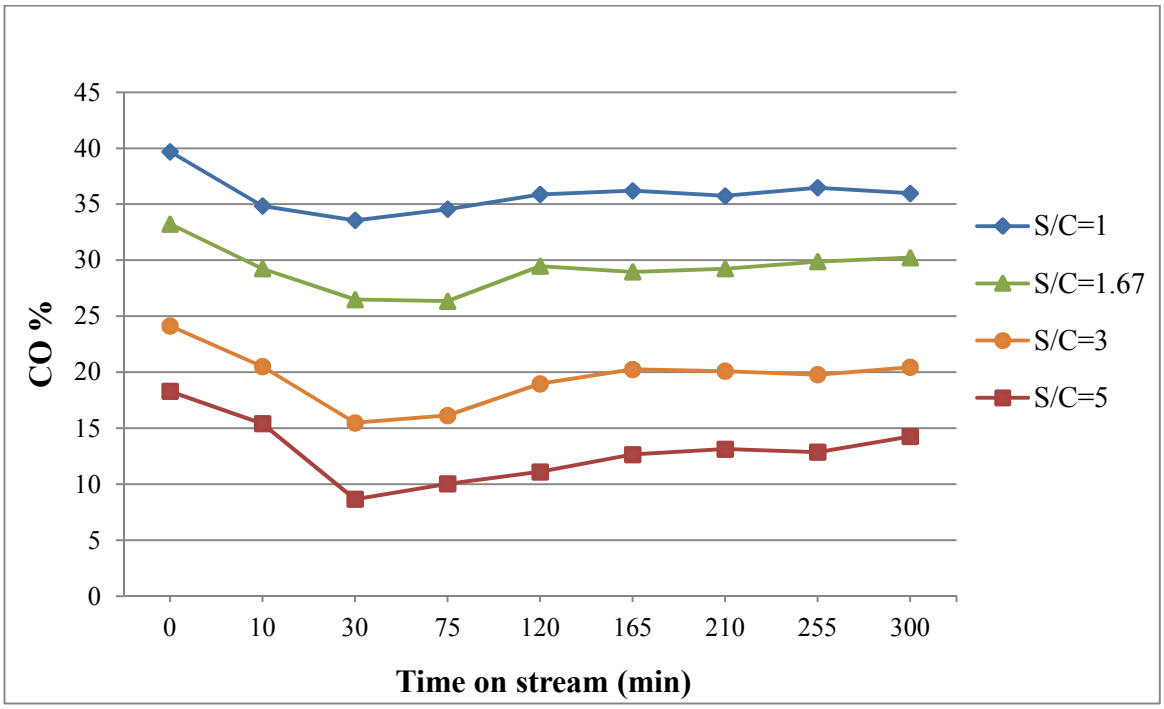

Figure 4.3. CO Content in the Product Stream during Reaction over Pd/CeO_2 at 300 °C.

The product compositions measured by gas chromatographs are listed in Table 4.1 and it is seen that CO_2 and H_2 concentration increase regularly with increasing temperature and S/C. Although WGS is an equimolar reaction, it is detected that H_2 concentration is somehow higher than CO_2 concentration. These finding is in agreement with the study of Chen *et al*. (2008). As a reason of this, they address the water decomposition reaction, which may occur under WGS reaction conditions. It is also reported that water decomposition becomes more significant with temperature. Results in Table 4.1 show that the difference between H_2 and CO_2 compositions becomes higher with temperature. This finding also supports the fact that water decomposition plays an important role.

Table 4.1. Product compositions (in dry basis) for 1.5%Pd/CeO_2 catalyst.

#	Temp.(°C)	S/C	CO Feed %	Product compositions		
				CO %	H_2 %	CO_2 %
1	250	1	40.7	38.5	1.8	1.7
2	250	1.67	33.2	31.3	2.2	1.9
3	250	3	25.1	22.8	2.3	2.1
4	250	5	18.0	15.8	2.5	2.2
5	300	1	39.7	36.1	3.4	2.9
6	300	1.67	33.2	29.6	3.6	3.3
7	300	3	24.1	19.9	4.9	4.3
8	300	5	18.3	13.2	5.5	4.7
9	325	1	39.7	34.0	5.6	5.0
10	325	1.67	33.74	25.4	7.3	6.4
11	325	3	25.2	15.9	8.5	7.7
12	325	5	18.6	8.9	9.3	8.2

In the second part of this study two different catalysts were prepared to examine the effect of the catalyst support material on CO conversion. 1.5wt.%Pd/TiO_2 catalyst was prepared by incipient to wetness impregnation method and 1.5wt.%Pd-20wt.%CeO_2/Al_2O_3 catalyst was synthesized by sequential incipient to wetness impregnation technique. These catalysts were tested for WGS reaction at 300 °C with S/C ratios of 1, 1.67, 3 and 5.

Similar to Pd/CeO_2 experiments total flow rate and N_2 flow rate kept constant at 70 and 30 $ml.min^{-1}$, respectively and the CO and H_2O feed compositions are given in Table 3.6. The results are compared with the CO conversion values obtained from Pd/CeO_2 catalyst at 300 °C and shown in Figure 4.4.

Pd/TiO_2 catalyst was tested for two S/C values, 1 and 3, and no activity was observed at this catalyst. The activity of $Pd\text{-}CeO_2/Al_2O_3$ catalyst was investigated with S/C ratios of 1, 1.67, 3 and 5. When compared with Pd/CeO_2 catalyst, $Pd\text{-}CeO_2/Al_2O_3$ exhibits less activity than Pd/CeO_2 catalyst and the difference becomes more notable at higher S/C ratios (Figure 4.4).

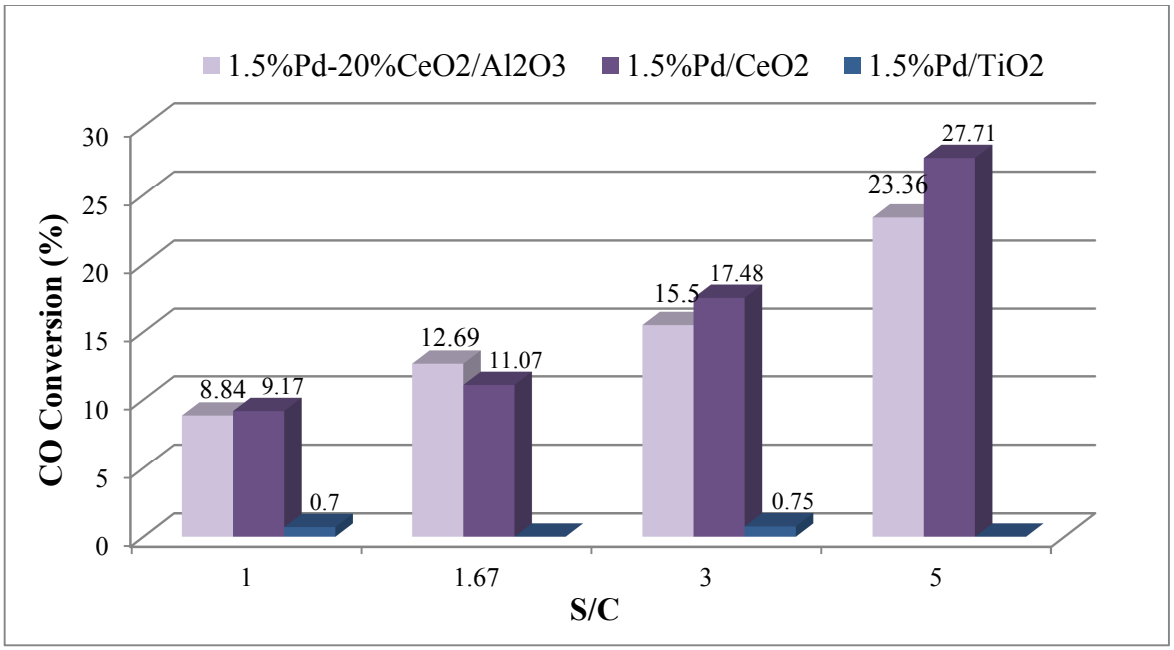

Figure 4.4. The Effect of Catalyst Support on CO Conversion (Temperature: 300 °C).

The product compositions for $Pd\text{-}CeO_2/Al_2O_3$ and Pd/TiO_2 catalysts are given in Table 4.2 and it is seen that H_2 and CO_2 concentrations in the product stream are less than those obtained from Pd/CeO_2 catalyst. Figure 4.5 shows the changes in CO content of the product and after sharp decline after 10 minutes, the steady state was reached after approximately 75 minutes.

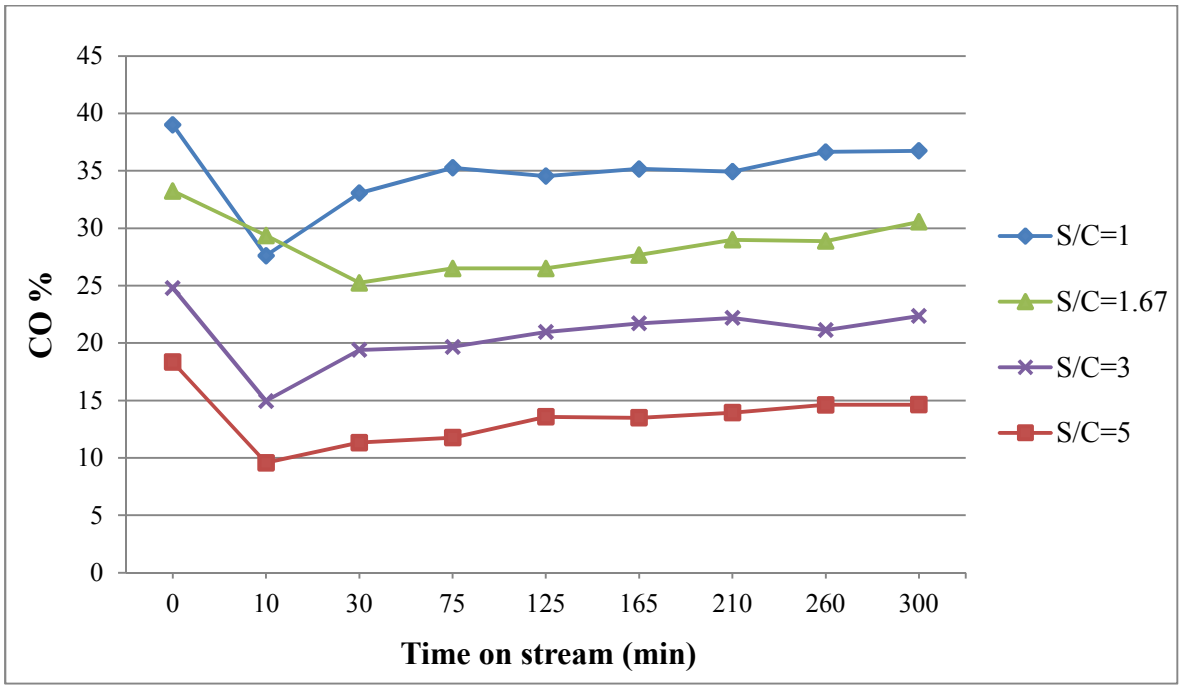

Figure 4.5. CO Content in the Product Stream during Reaction over Pd-CeO_2/Al_2O_3 at 300 °C.

Table 4.2. Product compositions (in dry basis) from WGS at 300 °C for 1.5%Pd-20%CeO_2/Al_2O_3 and 1.5%Pd/TiO_2 catalysts.

#	Catalyst	S/C	CO Feed %	Product compositions		
				CO %	H_2 %	CO_2 %
13	1.5%Pd-20%CeO_2/Al_2O_3	1	39.0	35.6	2.8	2.5
14	1.5%Pd-20%CeO_2/Al_2O_3	1.67	33.3	29.0	4.1	3.7
15	1.5%Pd-20%CeO_2/Al_2O_3	3	25.5	21.5	3.5	3.2
16	1.5%Pd-20%CeO_2/Al_2O_3	5	18.3	14.1	4.5	3.9
17	1.5%Pd/TiO_2	1	39.6	39.3	0.7	0.7
18	1.5%Pd/TiO_2	3	24.6	24.4	0.4	0.4

4.1.1. Catalyst Characterization

Characterization of the Pd/CeO_2 and Pd-CeO_2/Al_2O_3 catalysts are conducted by scanning electron microscopy (SEM) and energy dispersive X-ray spectroscopy (EDX)

analyses. To understand the effect of S/C ratio on catalyst structure, catalyst samples reacted at S/C=1 and 5 at 300 °C are tested under SEM and compared with the reduced samples' SEM micrographs.

SEM images of the reduced Pd/CeO_2 and $Pd\text{-}CeO_2/Al_2O_3$ catalysts are presented in Figure 4.6 and Figure 4.7. Heavy elements, like reduced metals, appear as bright spots, whereas lighter elements appear in dark. In Figure 4.7 darker areas represent Al_2O_3 sites; however Ce and Pd sites can not been distinguished in both catalyst samples; therefore metal dispersions are examined by EDX/Mapping analyses.

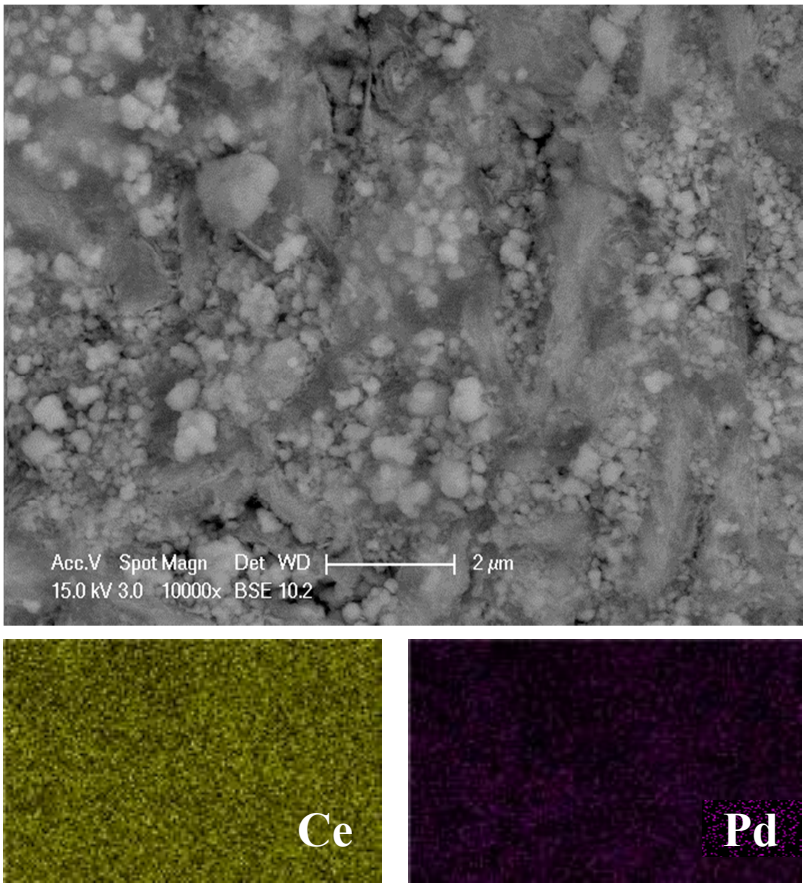

Figure 4.6. Backscattering Electron (BSE) SEM Micrographs and Ce and Pd Mappings of Reduced Pd/CeO_2 Catalyst. Magnification is 10000x.

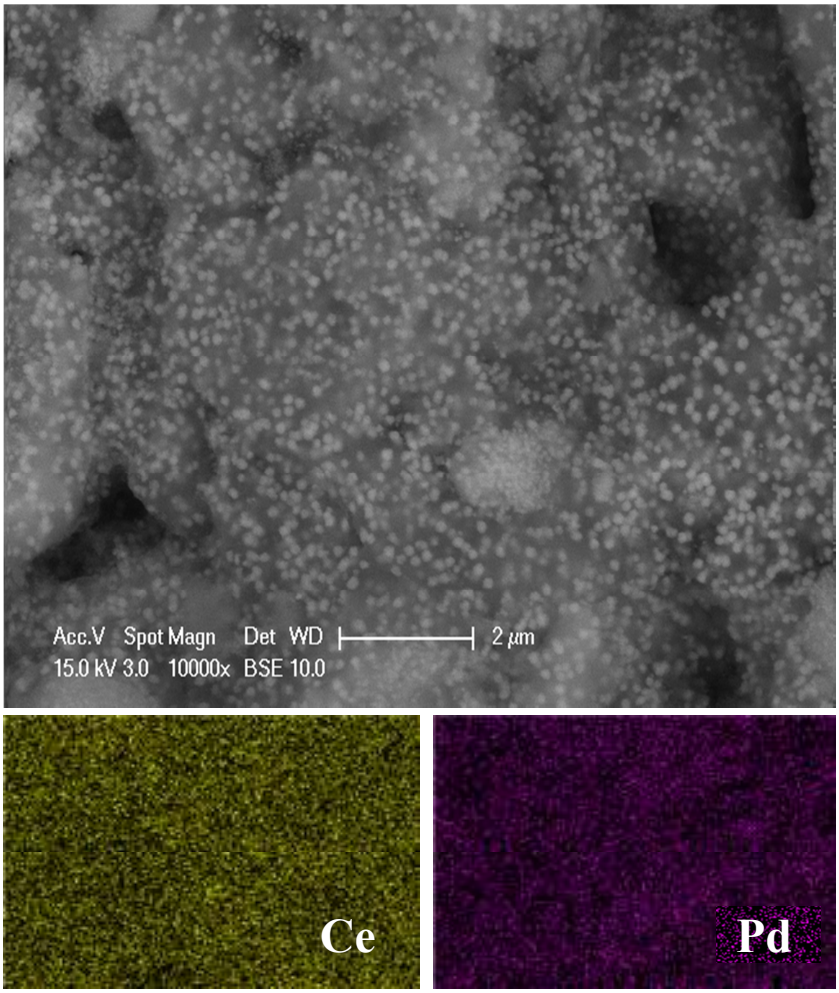

Figure 4.7. Backscattering Electron (BSE) SEM Micrographs and Ce and Pd Mappings of Reduced Pd-CeO_2/Al_2O_3 Catalyst. Magnification is 10000x.

EDX/Mapping images show that almost uniform Pd dispersion is obtained for each catalyst. The metal loading of the catalysts are determined by EDX analysis and the results are expressed by taking the average of the results obtained from five samples out of the same batch, either reduced or spent (Table 4.3).

Table 4.3. SEM/EDX results for the metal contents of the catalysts.

Catalyst	**Metal**	**Average metal wt%**	**Target**
Pd/CeO_2	Pd	1.66	1.5
Pd-CeO_2/Al_2O_3	Pd	2.18	1.5
	Ce	21.96	16

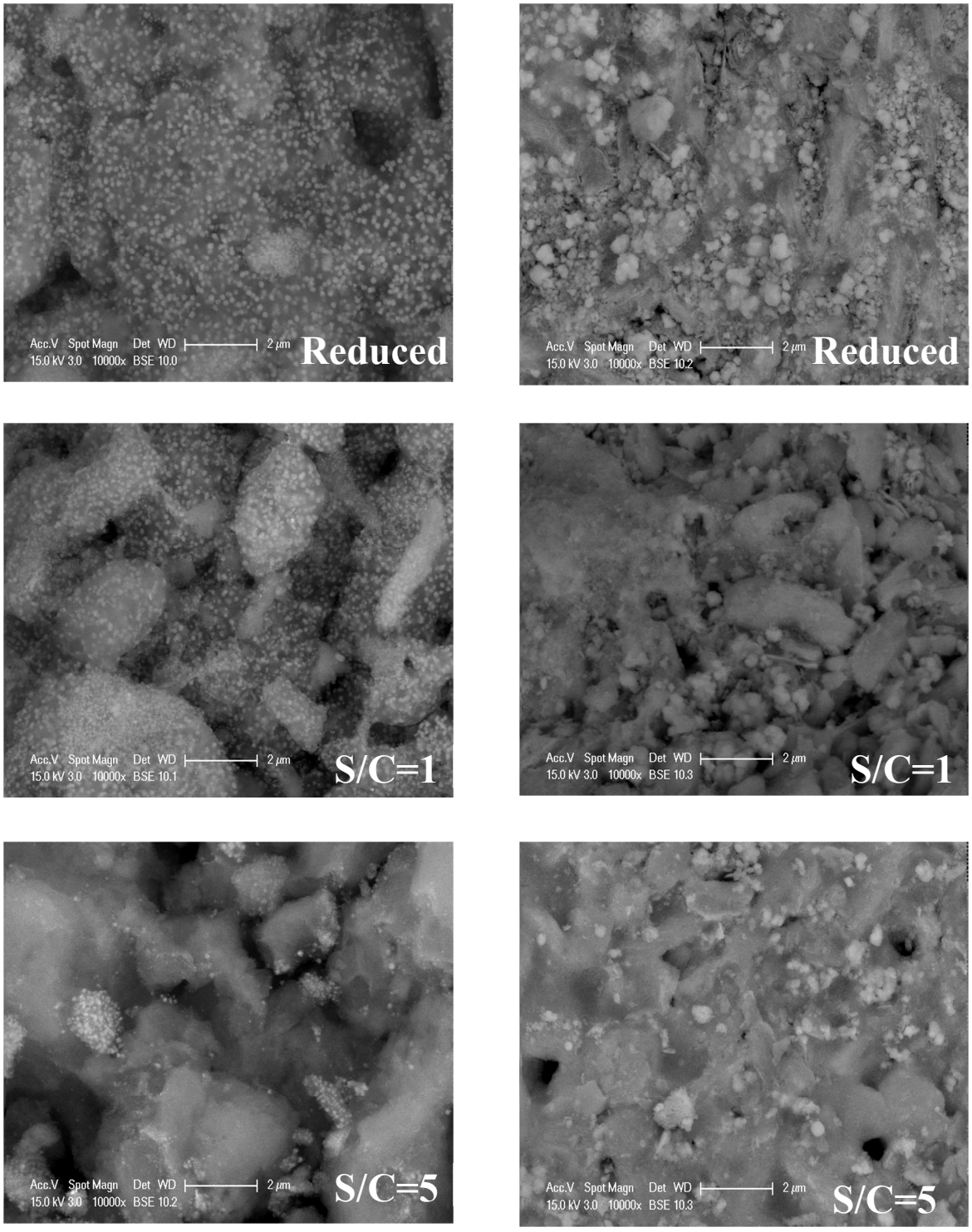

(a) (b)

Figure 4.8. Backscattering Electron (BSE) SEM Micrographs of Reduced and Reacted Catalysts. a. Pd-CeO_2/Al_2O_3 b. Pd/CeO_2 (Magnification is 10000x.)

SEM micrographs of reduced and reacted catalysts are given in Figure 4.8. Since Pd and Ce metals cannot be distinguished, it is hard to observe the changes in metal dispersion and catalyst surface on Pd/CeO_2 catalyst samples. On the other hand, agglomeration of Pd-Ce clusters is detected on $Pd\text{-}CeO_2/Al_2O_3$ catalyst reacted at 300 °C, S/C=5, which results in loss of surface area and this can be the reason of higher CO conversion differences between Pd/CeO_2 and $Pd\text{-}CeO_2/Al_2O_3$ at this reaction condition. No coke formation is observed on each spent catalysts by SEM and EDX analyses.

4.2. WGS in Packed Microchannel

The second section of this study involves the investigation of the impact of reactor geometry on CO conversion. WGS reaction experiments were conducted over 1.5wt.%Pd/CeO_2 catalyst in microchannel reactor with dimensions explained in Sections 3.3.4 and 3.4.3.

Firstly, it was aimed to conduct WGS in wall-coated microchannel reactor. CeO_2 support with particle size above 100 mesh was used for 1.5%Pd/CeO_2 preparation and the catalyst was coated on FeCrAlY plate by blade-coating method described in Section 3.3.4. Each plate included 10 mg catalyst and this microchannel configuration was tested for WGS at 325 °C and S/C=5. At several attempts it was observed that the adhesion between the ceria supported catalyst and FeCrAlY plate was not strong enough to endure reaction conditions. Goerke *et al*. (2004) also indicated that the ceria supported catalysts stick relatively weakly on plates, when compared to Fe_2O_3 and ZrO_2 supported catalysts. This test reveals that the coating method used in this research is not suitable for preparing wall-coated CeO_2 supported catalysts.

In order to understand the effect of reactor structure on CO conversion, WGS experiments were performed in particulate microchannel reactor described in Section 3.4.3. The catalyst used in these experiments is 1.5wt.%Pd/CeO_2 with 60-80 mesh particle size to provide uniform flow distribution. The effect of reaction temperature and S/C ratios were examined and compared with the results obtained from Pd/CeO_2 catalysts' in conventional packed bed reactor. The microchannel was packed with 20 mg catalyst and WGS was tested at 300 and 325 °C, with S/C ratios 1, 1.67, 3 and 5. The total flow and N_2 flow were

kept fixed at 70 and 30 ml.min^{-1}, respectively and the other feed compositions are given in Table 3.7. The obtained results are presented in Figures 4.9 and 4.10. Since the reactors involved different amount catalyst the comparison is made in terms of reactor productivity (Equation 4.1).

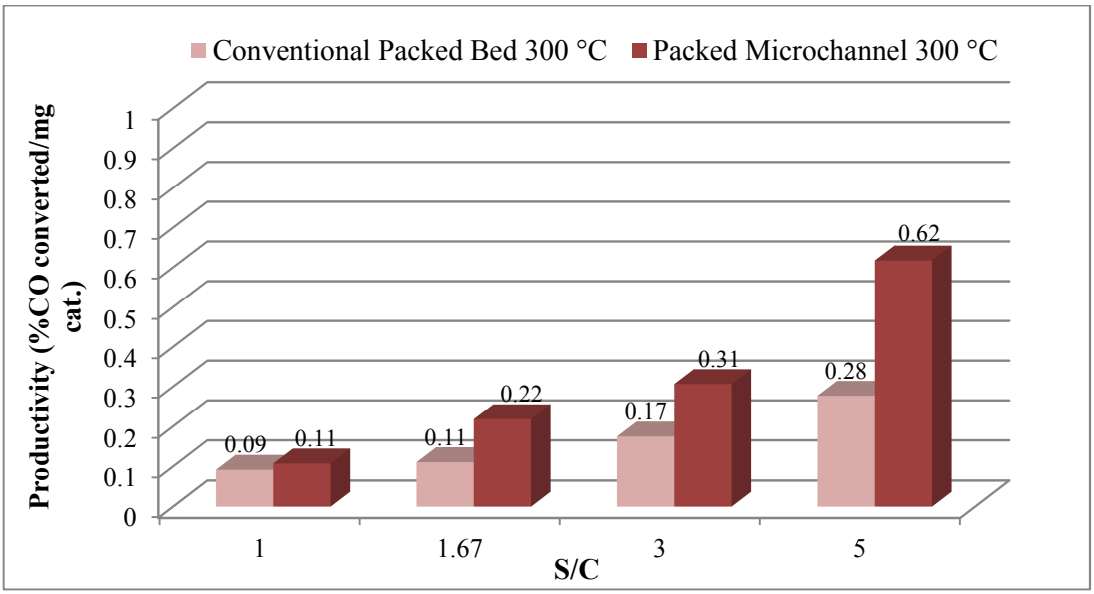

Figure 4.9. The Catalyst Productivity in Conventional Packed Bed and Packed Microchannel Reactors at 300 °C.

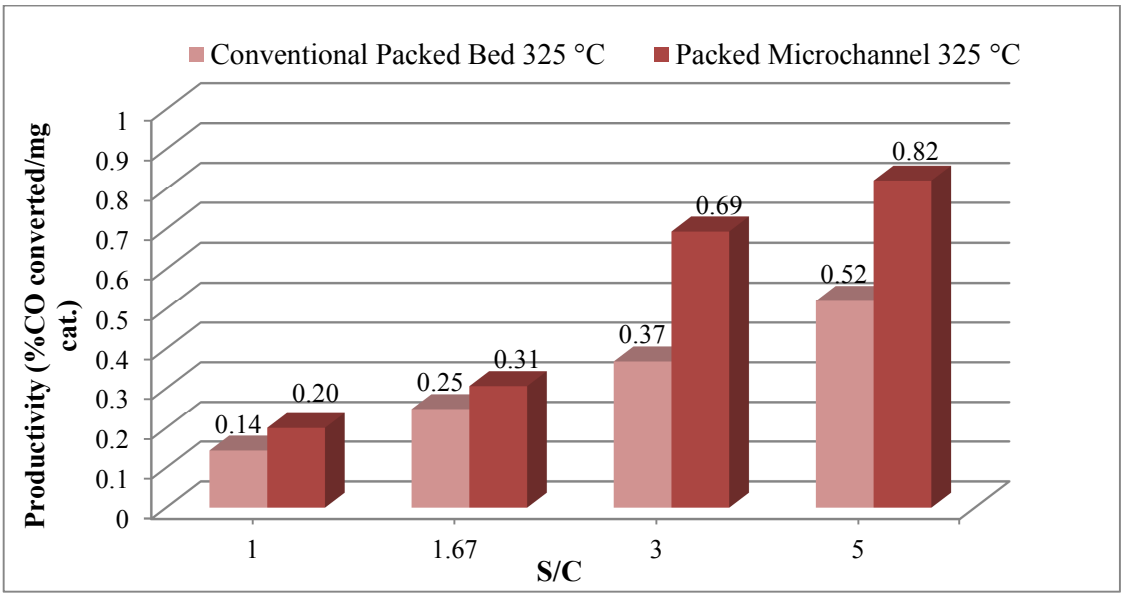

Figure 4.10. The Catalyst Productivity in Conventional Packed Bed and Packed Microchannel Reactors at 325˚C.

Increasing temperature and S/C enhance the catalyst activity also in the packed microchannel reactor. The product compositions obtained from the experiments are given in Table 4.4 and increase in CO_2 and H_2 compositions is observed at higher reaction temperatures and S/C ratios. Comparisons of the results show that, under the same reaction conditions microchannel reactor configuration with less amount of catalyst exhibits better productivity than the conventional packed bed performance. Possible reasons of the findings reported above are thought to be the better heat transfer and flow distribution characteristics of the microchannel reactors. Microchannel geometry employed in this study allows effective transfer of external heat to the catalyst bed, and, as a result WGS reaction is favored to deliver higher CO conversions. L/dp (L: catalyst bed height, dp: average particle diameter) ratios are calculated for both reactor configurations. For conventional packed bed reactor L/dp ratio is found to be 13.3, while microchannel reactor configuration reached 22.5. Since L/dp ratio is significantly higher for microchannel reactor, it can be concluded that flow distribution is better in microchannel configuration.

The differences between the conventional packed bed and microchannel configuration have not been attributed to particle size. The previous WGS studies conducted by CATREL research group showed that 45-60 particle mesh size is free from the effect of intraparticle transport resistance. Therefore it is concluded that using 45-60 or 60-80 particle size does not cause intraparticle transport resistance.

The changes in CO content in product stream are presented in Figures 4.11 and 4.12. At 300 °C, the steady state was reached faster at microchannel than conventional packed bed reactor system, approximately after 75 minutes. At 325 °C, especiallly at higher S/C ratios steady state was reached after 165 minutes.

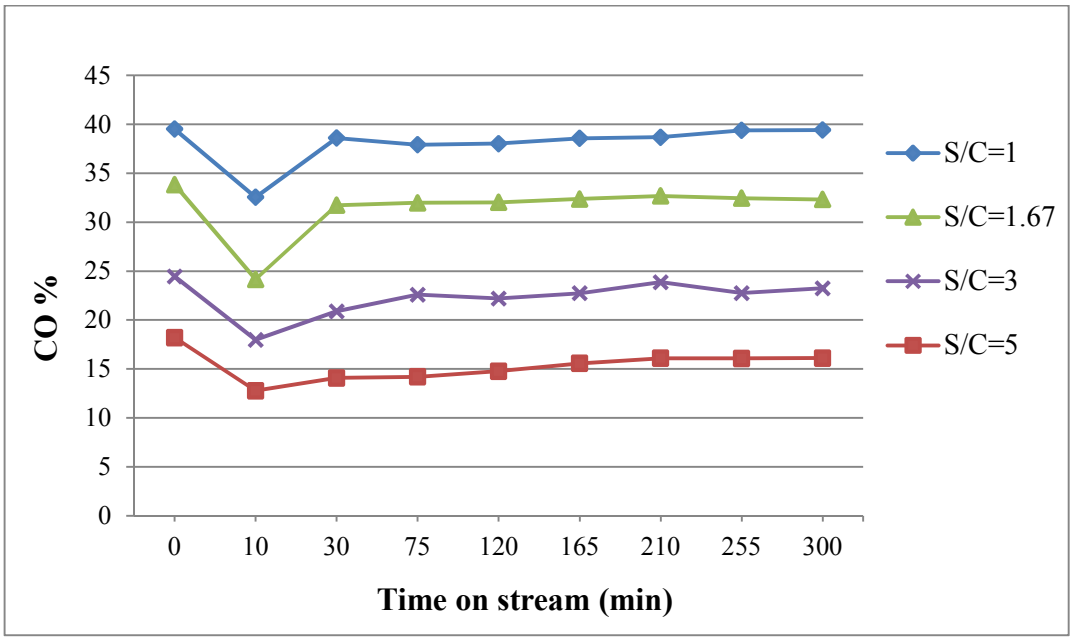

Figure 4.11. CO Content in the Product Stream during Reaction over Pd/CeO_2 in Packed Microchannel at 300 °C.

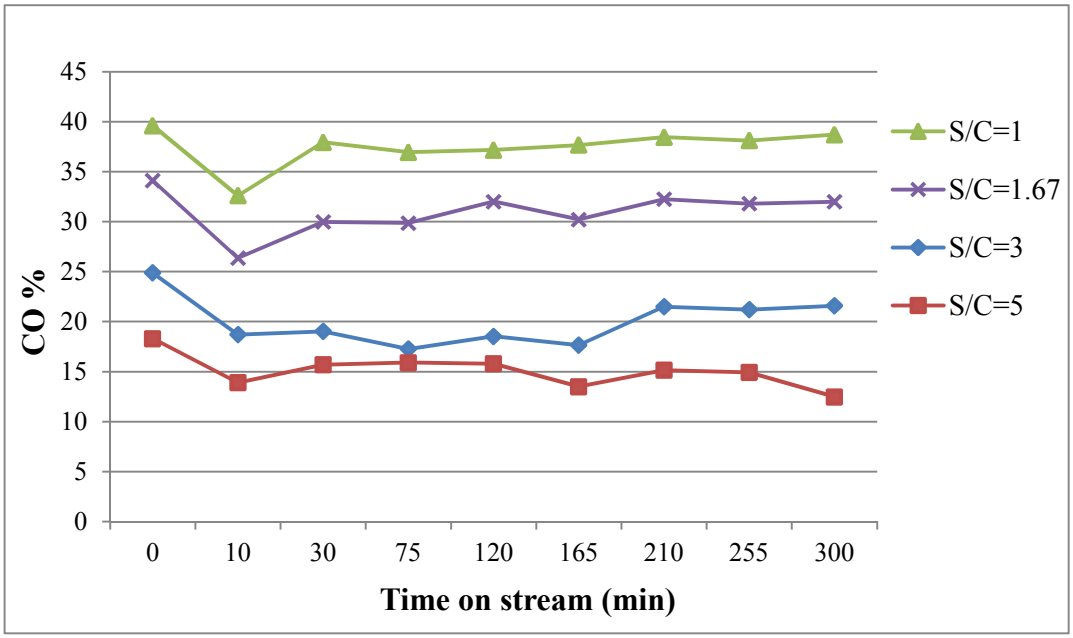

Figure 4.12. CO Content in the Product Stream during Reaction over Pd/CeO_2 in Packed Microchannel at 325 °C.

Table 4.4. Product compositions (in dry basis) for 1.5%Pd/CeO_2 catalyst in packed microchannel.

#	Temp.(°C)	S/C	CO Feed %	Product compositions		
				CO %	H_2 %	CO_2 %
19	300	1	39.5	38.7	0.9	0.9
20	300	1.67	33.8	32.4	1.0	0.9
21	300	3	24.5	23.0	1.7	1.5
22	300	5	18.2	16.0	2.4	2.1
23	325	1	39.6	38.0	1.4	1.3
24	325	1.67	34.1	32.0	1.9	1.7
25	325	3	24.9	21.4	3.8	3.4
26	325	5	18.3	15.3	3.5	3.2

5. CONCLUSIONS AND RECOMMENDATIONS

5.1. Conclusions

The major objective of this study was to perform parametric investigations of Pd based catalysts driven WGS reaction and explore the effect of the reactor structuring and the catalyst support on CO conversion. The experiments were conducted at several reaction temperatures and S/C ratios in conventional fixed bed and packed microchannel reactors. The following conclusions that can be drawn from this research can be given as follows:

- Experimental studies revealed that for each catalyst type and reactor structure studied in this research, increasing the reaction temperature and S/C ratio in the feed enhanced CO conversion.

- In addition to the type of the active metal, the catalytic activity also depends on the catalyst support material. Among the catalysts investigated, 1.5wt.%Pd/CeO_2 exhibited the best performance in terms of CO conversion.

- SEM/EDX analysis showed that almost homogeneous dispersion of Pd was achieved for Pd/CeO_2 and Pd-CeO_2/Al_2O_3 catalysts. The analysis also revealed that when these catalysts exposed to WGS reaction conditions, no coke formation occurred.

- Agglomeration of active metal sites was observed only on the Pd-CeO_2/Al_2O_3 catalyst reacted at S/C=5, which might be the reason of low WGS activity of this catalyst.

- When compared to conventional packed bed configuration, packed microchannel reactor exhibited much better productivity, even though it involved less amount of catalyst.

5.2. Recommendations

The following recommendations are thought to be beneficial for possible future studies to improve this research:

- The WGS reaction can be studied over ceria supported Pd catalysts under real reformate conditions. Hence the effect of the product in the feed on CO conversion can be determined.

- Coating of CeO_2 based Pd catalyst to FeCrAlY support requires further investigation. Other coating techniques, like sol-gel method, can be applied to ceria supported catalysts for preparing wall-coated microchannels.

- More parametric studies can be carried out in a wide range of temperature over Pd-CeO_2/Al_2O_3 catalyst, considering that it exhibited CO conversions close to Pd/CeO_2 values at low S/C ratios.

- Longer time-on-stream tests can be performed over Pd-CeO_2/Al_2O_3 and Pd/CeO_2 catalysts to examine their stability.

APPENDIX A: CALIBRATION OF MASS FLOW CONTROLLERS

Calibration curves of the Brooks mass flow controllers used in the experiments are given below.

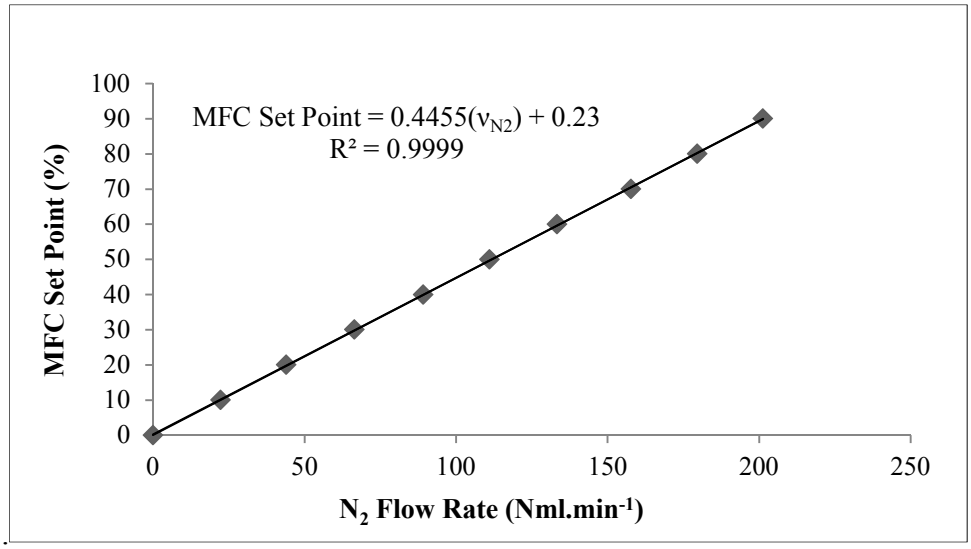

Figure A.1. Calibration Curve of the Nitrogen Mass Flow Controller.

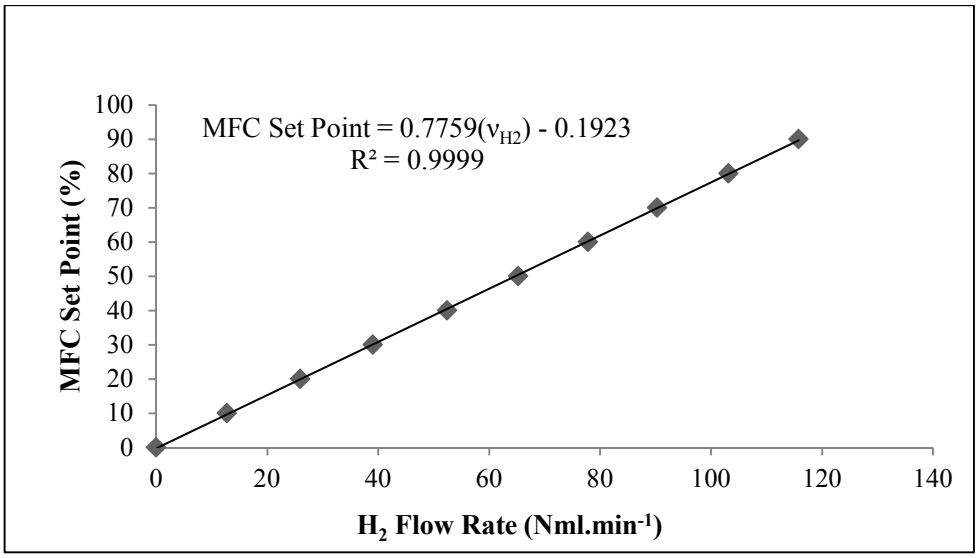

Figure A.2. Calibration Curve of the Hydrogen Mass Flow Controller.

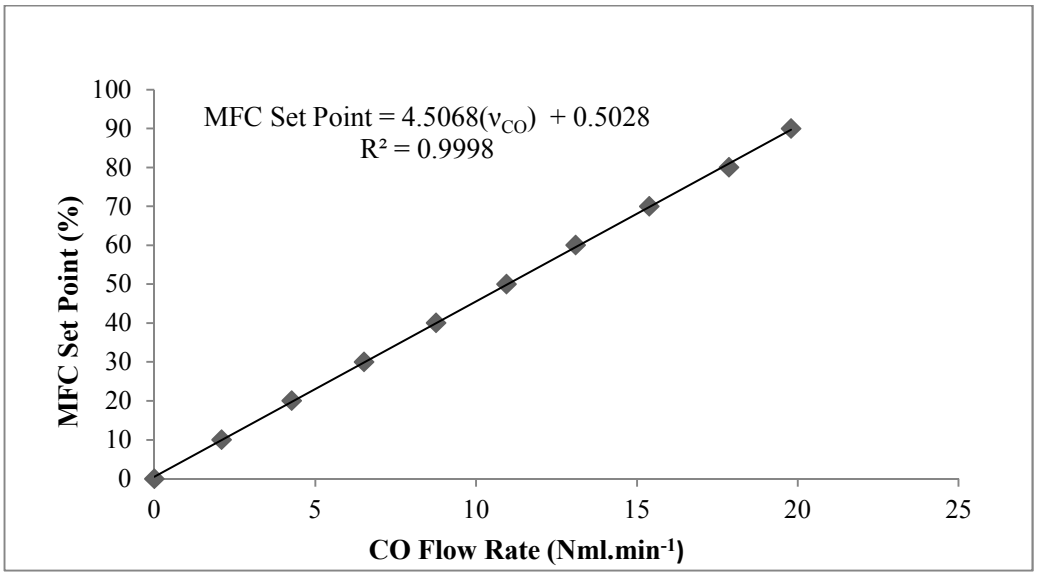

Figure A.3. Calibration Curve of the Carbon Monoxide Mass Flow Controller.

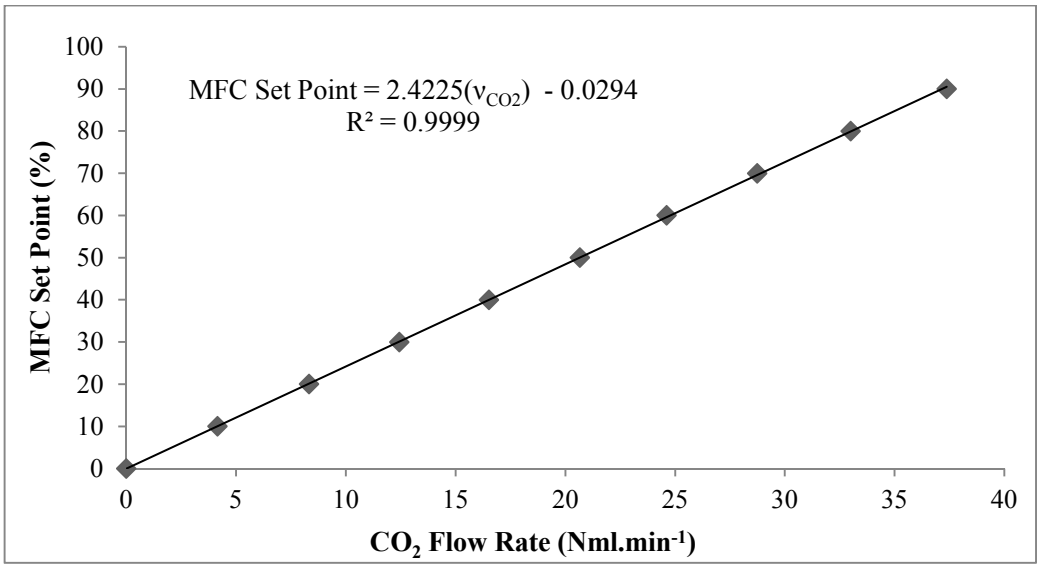

Figure A.4. Calibration Curve of the Carbon Dioxide Mass Flow Controller.

APPENDIX B: CALIBRATION OF THE GAS CHROMATOGRAPHS

Calibration curves of gases analyzed at HP Agilent 6890N gas chromatograph are given below.

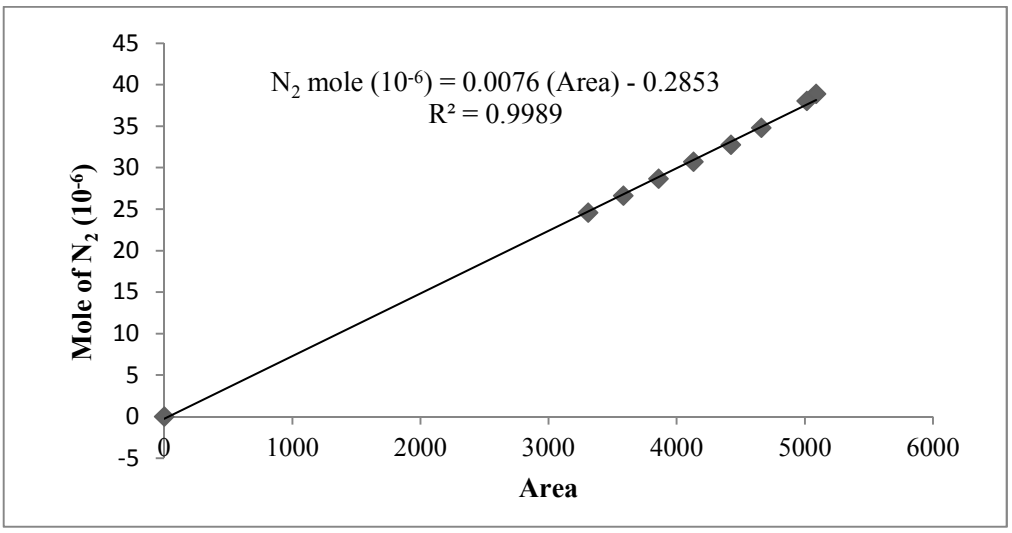

Figure B.1. GC Calibration Curve for Nitrogen.

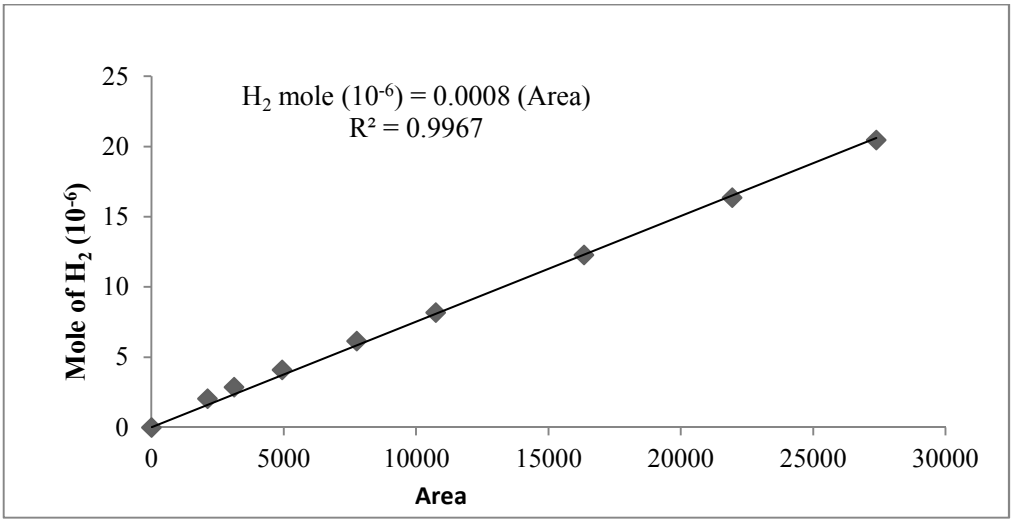

Figure B.2. GC Calibration Curve for Hydrogen.

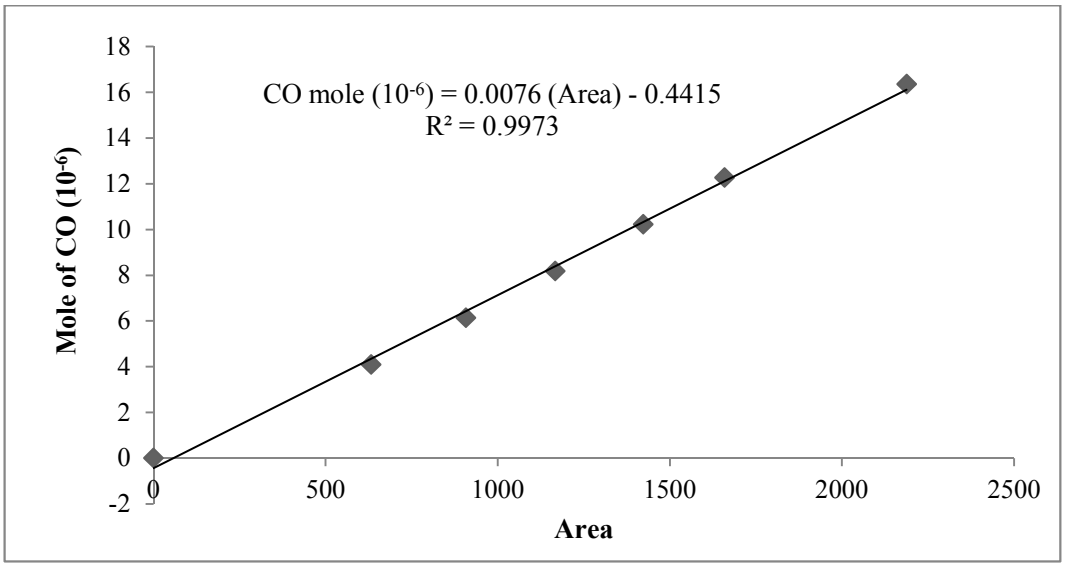

Figure B.3. GC Calibration Curve for Carbon Monoxide.

Calibration curves of gases analyzed at HP Agilent 6850N gas chromatograph are given below.

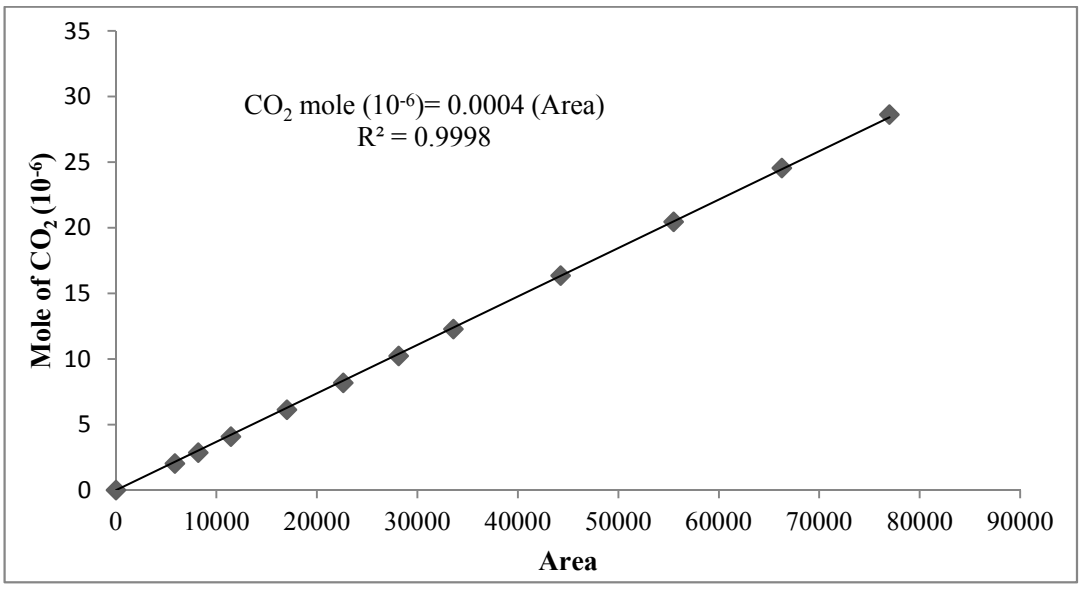

Figure B.4. GC Calibration Curve for Carbon Dioxide.

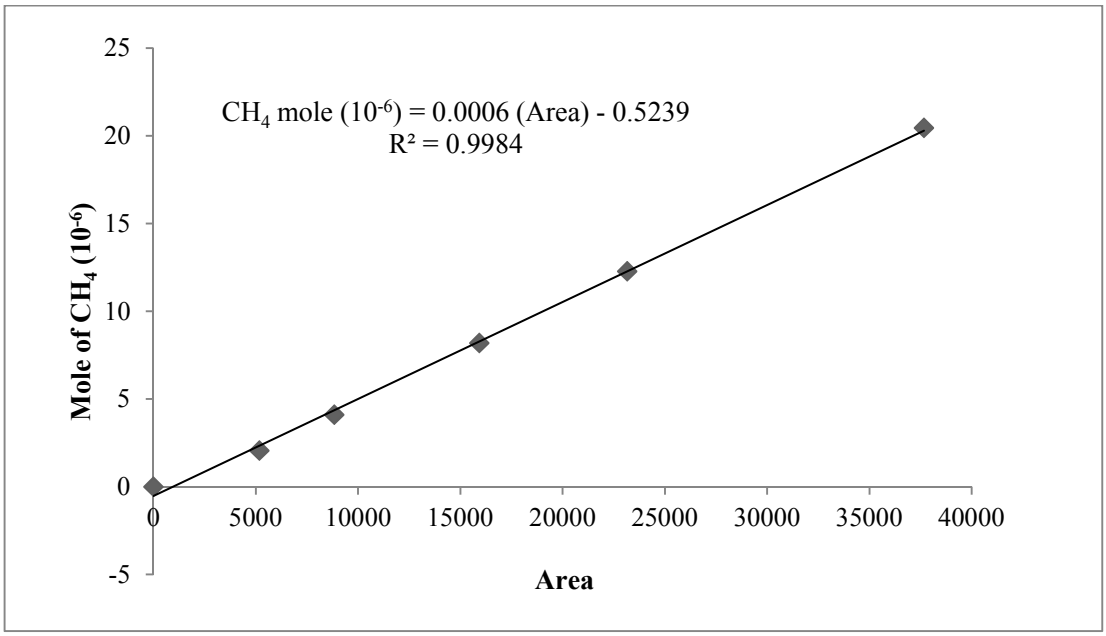

Figure B.5. GC Calibration Curve for Methane.

REFERENCES

Aktürk, N., 2011, *Catalyst Screening and Testing for Steam Reforming of Methane to Synthesis Gas*, M.S. Thesis, Boğaziçi University.

Amadeo, N. E., and M. A. Laborde, 1995, "Hydrogen Production from the Low-Temperature Water-Gas Shift Reaction: Kinetics and Simulation of the Industrial Reactor", *International Journal of Hydrogen Energy*, Vol. 20, No. 12, pp. 949-956.

Andreeva, D., V. Idakiev, T. Tabakova, L. Ilievaa, P. Falaras, A. Bourlinos, and A. Travlos, 2002, "Low-Temperature Water-Gas Shift Reaction over Au/CeO_2 Catalysts", *Catalysis Today*, Vol. 72, pp. 51-57.

Baier, T., and G. Kolb, 2007, "Temperature Control of the Water Gas Shift Reaction in Microstructured Reactors", *Chemical Engineering Science*, Vol. 62, pp. 4602-4611.

BASF Catalysts, 2014, *Engelhard Industrial Bullion Prices*, http://apps.catalysts.basf.com/apps/eibprices/mp, accessed at June 2014.

Boaro, M., M. Vicario, J. Llorca, C. Leitenburg, G. Dolcetti, and A. Trovarelli, 2009, "A Comparative Study of Water Gas Shift Reaction over Gold and Platinum Supported on ZrO_2 and CeO_2–ZrO_2", *Applied Catalysis B: Environmental*, Vol. 88, pp. 272-282.

Buitrago, R., J. Ruiz-Martínez, J. Silvestre-Albero, A. Sepúlveda-Escribano, and F. Rodríguez-Reinoso, 2012, "Water Gas Shift Reaction on Carbon-Supported Pt Catalysts Promoted by CeO_2", *Catalysis Today*, Vol. 180, pp. 19-24.

Bunluesin, T., R. J. Gorte, and G. W. Grahamb, 1998, "Studies of the Water-Gas-Shift Reaction on Ceria-Supported Pt, Pd, and Rh: Implications for Oxygen-Storage Properties", *Applied Catalysis B: Environmental*, Vol. 15, pp. 107-114.

Callaghan, C. A., 2006, *Kinetics and Catalysis of the Water-Gas-Shift Reaction: A Microkinetic and Graph Theoretic Approach*, Ph.D. Thesis, Worcester Polytechnic Institute.

Chen, W. H., and J. G. Jheng, 2007, "Characterization of Water Gas Shift Reaction in Association with Carbon Dioxide Sequestration", *Journal of Power Sources*, Vol. 172, pp. 368-375.

Chen, W. H., T. C. Hsieh, and T. L. Jiang, 2008, "An Experimental Study on Carbon Monoxide Conversion and Hydrogen Generation from Water Gas Shift Reaction", *Energy Conversion and Management*, Vol. 49, pp. 2801-2808.

Choi, Y., and H. G. Stenger, 2003, "Water Gas Shift Reaction Kinetics and Reactor Modeling for Fuel Cell Grade Hydrogen", *Journal of Power Sources*, Vol. 124, pp. 432–439.

Colussi, S., L. Katta, F. Amoroso, R. J. Farrauto, and A. Trovarelli, 2014, "Ceria-Based Palladium Zinc Catalysts as Promising Materials for Water Gas Shift Reaction", *Catalysis Communications*.

Cornaglia, C. A., J. F. Munera, and E. A. Lombardo, 2011, "Kinetic Study of a Novel Active and Stable Catalyst for the Water Gas Shift Reaction", *Industrial & Engineering Chemistry Research*, Vol. 50, pp. 4381-4389.

Dagle, R. A., A. Platon, D. R. Palo, A. K. Datye, J. M. Vohs, and Y. Wang, 2008, "PdZnAl Catalysts for the Reactions of Water-Gas-Shift, Methanol Steam Reforming and Reverse-Water-Gas-Shift", *Applied Catalysis A: General*, Vol. 342, pp. 63-68.

Deshpande, P. A., M. S. Hegde, and G. Madras, 2010, "A Mechanistic Model for the Water-Gas Shift Reaction over Noble Metal Substituted Ceria", *American Institute of Chemical Engineers*, Vol. 56, pp. 1315-1324.

Ehrfeld, W., V. Hessel, and H. Löwe, 2000, Microreactors: New Technology for Modern Chemistry**,** WILEY-VCH Verlag GmbH, Weinheim, Germany.

Galvita, V., T. Schröder, B. Munder, and K. Sundmacher, 2008, "Production of Hydrogen with Low CO_x-Content for PEM Fuel Cells by Cyclic Water Gas Shift Reactor", *International Journal of Hydrogen Energy,* Vol. 33, pp. 1354-1360.

Germani, G., P. Alphonse, M. Courty, Y. Schuurman, and C. Mirodatos, 2005, "Platinum/Ceria/Alumina Catalysts on Microstructures for Carbon Monoxide Conversion", *Catalysis Today*, Vol. 110, pp. 114-120.

Goerke, O., P. Pfeifer, and K. Schubert, 2004, "Water Gas Shift Reaction and Selective Oxidation of CO in Microreactors", *Applied Catalysis A: General*, Vol. 263, pp. 11-18.

Gorte, R. J., and S. Zhao, 2005, "Studies of the Water-Gas-Shift Reaction with Ceria-Supported Precious Metals", *Catalysis Today*, Vol. 104, pp. 18-24.

Hilaire, S., X. Wang, T. Luo, R. J. Gorte, and J. Wagner, 2001, "A Comparative Study of Water-Gas-Shift Reaction over Ceria Supported Metallic Catalysts", *Applied Catalysis A: General*, Vol. 215, pp. 271-278.

Holladay, J. D., J. Hu, D. L. King, and Y. Wang, 2009, "An Overview of Hydrogen Production Technologies", *Catalysis Today*, Vol. 139, pp. 244-260.

Jacobs, G., L. Williams, U. Graham, G. A. Thomas, D. E. Sparks, and B. H. Davis, 2003, "Low Temperature Water–Gas Shift: In Situ DRIFTS-Reaction Study of Ceria Surface Area on the Evolution of Formates on Pt/CeO_2 Fuel Processing Catalysts for Fuel Cell Applications", *Applied Catalysis A: General*, Vol. 252, pp. 107–118.

Karakaya, M., 2012, *Experimental and Quantitative Analysis of Multiphase Catalytic Reactions under Microfluidic Flow Conditions and Geometries,* Ph.D. Thesis**,** Boğaziçi University.

Kim, Y. T., E. D. Park, H. C. Lee, D. Lee, and K. H. Lee, 2009, "Water-Gas Shift Reaction over Supported Pt-CeO_x Catalysts", *Applied Catalysis B: Environmental*, Vol. 90, pp. 45-54.

Kirubakaran, A., S. Jain, and R. K. Nema, 2009, "A Review on Fuel Cell Technologies and Power Electronic Interface", *Renewable and Sustainable Energy Reviews*, Vol. 13, pp. 2430-2440.

Kiwi-Minsker, L., and A. Renken, 2005, "Microstructured Reactors for Catalytic Reactions", *Catalysis Today*, Vol. 110, pp. 2-14.

Kolb, G., H. Pennemann, and R. Zapf, 2005, "Water-Gas Shift Reaction in Micro-Channels—Results from Catalyst Screening and Optimisation", *Catalysis Today*, Vol. 110, pp. 121-131.

Koryabkina, N. A., A. A. Phatak, W. F. Ruettinger, R. J. Farrauto, and F. H. Ribeiro, 2003, "Determination of Kinetic Parameters for the Water–Gas Shift Reaction on Copper Catalysts under Realistic Conditions for Fuel Cell Applications", *Journal of Catalysis*, Vol. 217, pp. 233-239.

Kugai, J., J. T. Miller, N. Guo, and C. Song, 2011, "Role of Metal Components in Pd–Cu Bimetallic Catalysts Supported on CeO_2 for the Oxygen-Enhanced Water Gas Shift", *Applied Catalysis B: Environmental*, Vol. 105, pp. 306-316.

Kušar, H., S. Hočevar, and J. Levec, 2006, "Kinetics of the Water–Gas Shift Reaction over Nanostructured Copper–Ceria Catalysts", *Applied Catalysis B: Environmental*, Vol. 63, pp. 194-200.

Ladebeck, J. R., and J. P. Wagner, 2003, "Catalyst Development for Water-Gas Shift", *Handbook of Fuel Cells – Fundamentals, Technology and Applications,* Vol. 3, Part. 2, pp. 190-211.

Lee, C. H., and Y. W. Chen, 1998, "Effect of Additives on Pd/Al_2O_3 for CO and Propylene Oxidation at Oxygen-Deficient Conditions", *Applied Catalysis B: Environmental*, Vol. 17, pp. 279-291.

Lenite, B. A., C. Galletti, and S. Specchia, 2011, "Studies on Au Catalysts for Water Gas Shift Reaction", *International Journal of Hydrogen Energy*, Vol. 39, pp. 7750-7758.

Li, Y., Q. Fu, and M. Flytzani-Stephanopoulos, 2000, "Low-Temperature Water-Gas Shift Reaction over Cu and Ni Loaded Cerium Oxide Catalysts", *Applied Catalysis B: Environmental*, Vol. 27, pp.179-191.

Mills, P. L., D. J. Quiram, and J. F. Ryley, 2007, "Microreactor Technology and Process Miniaturization for Catalytic Reactions—A Perspective on Recent Developments and Emerging Technologies", *Chemical Engineering Science*, Vol. 62, pp. 6992-7010.

Noor, T., M. V. Gil, and D. Chen, 2014, "Production of Fuel-Cell Grade Hydrogen by Sorption Enhanced Water Gas Shift Reaction Using Pd/Ni–Co Catalysts", *Applied Catalysis B: Environmental*, Vol. 150, No. 151, pp. 585-595.

Önsan, Z. İ., 2007, "Catalytic Processes for Clean Hydrogen Production from Hydrocarbons", *Turk J Chem*, Vol. 31, pp. 531-550.

Panagiotopoulou, P., and D. I. Kondarides, 2006, "Effect of the Nature of the Support on the Catalytic Performance of Noble Metal Catalysts for the Water–Gas Shift Reaction", *Catalysis Today*, Vol. 112, pp. 49-52.

Ratnasamy, C., and J. P. Wagner, 2009, "Water Gas Shift Catalysis", *Catalysis Reviews: Science and Engineering*, Vol. 51, No. 3, pp. 325-440.

Rhodes, C., B. P. Williams, F. King, and G. J. Hutchings, 2002, "Promotion of Fe_3O_4/ Cr_2O_3 High Temperature Water Gas Shift Catalyst", *Catalysis Communications*, Vol. 3, pp. 381-384.

Roh, H. S., H. S. Potdar, D. W. Jeong, K. S. Kim, J. O. Shim, W. J. Jang, K. Koo, and W. Y. Yoon, 2012, "Synthesis of Highly Active Nano-Sized (1wt.% Pt/CeO_2) Catalyst for Water Gas Shift Reaction in Medium Temperature Application", *Catalysis Today*, Vol. 185, pp. 113-118.

Sato, T., S. Kurosawa, R. L. Smith Jr., T. Adschiri, and K. Arai, 2004, "Water Gas Shift Reaction Kinetics Under Noncatalytic Conditions in Supercritical Water", *Journal of Supercritical Fluids*, Vol. 29, pp. 113-119.

Shido, T., and Y. Iwasawa, 1993, "Reactant-Promoted Reaction Mechanism for Water-Gas Shift Reaction on Rh-Doped CeO_2", *Journal of Catalysis*, Vol. 141, pp. 71-81.

Shinde, M. V., and G. Madras, 2012, "Water Gas Shift Reaction over Multi-Component Ceria Catalysts", *Applied Catalysis B: Environmental*, Vol. 123, No. 124, pp. 367-378.

Smith, B., M. Loganathan, and M. S. Shantha, 2010, "A Review of the Water Gas Shift Reaction Kinetics", *International Journal of Chemical Reactor Engineering*, Vol. 8.

Soria, M. A., P. Perez, S. A. C. Carabineiro, F. C. Maldonado-Hodar, A. Mendes, and L. M. Madeira, 2013, "Effect of the Preparation Method on the Catalytic Activity and Stability of Au/Fe_2O_3 Catalysts in the Low-Temperature Water-Gas Shift Reaction", *Applied Catalysis A: General.*

Şimsek, E., M. Karakaya, A. K. Avci, and Z. I. Önsan, 2013, "Oxidative Steam Reforming of Methane to Synthesis Gas in Microchannel Reactors", *International Journal of Hydrogen Energy*, Vol. 38, pp. 870-878.

Tonkovich, A. Y., S. Perry, Y. Wang, D. Qiu, T. La Plante, and W. A. Rogers, 2004, "Microchannel Process Technology for Compact Methane Steam Reforming", *Chemical Engineering Science*, Vol. 59, pp. 4819 – 4824.

Tonkovich, A., D. Kuhlmann, A. Rogers, J. McDaniel, S. Fitzgerald, R. Arora, and T. Yuschak, 2005, "Microchannel Technology Scale-Up to Commercial Capacity", *Chemical Engineering Research and Design*, Vol. 83, No. 6, pp. 634-639.

Trimm, D. L., 2005, "Minimisation of Carbon Monoxide in a Hydrogen Stream for Fuel Cell Application", *Applied Catalysis A: General*, Vol. 296, pp. 1-11.

Wang, X., R. J. Gorte, and J. P. Wagner, 2002, "Deactivation Mechanisms for Pd/Ceria during the Water–Gas-Shift Reaction", *Journal of Catalysis*, Vol. 212, pp. 225-230.

Wang, X., and R. J. Gorte, 2003, "The Effect of Fe and Other Promoters on the Activity of Pd/Ceria for the Water-Gas Shift Reaction*", Applied Catalysis A: General*, Vol. 247, pp. 157-162.

Yahiro, H., K. Murawaki, K. Saiki, T. Yamamoto, and H. Yamaura, 2007, "Study on the Supported Cu-Based Catalysts for the Low-Temperature Water–Gas Shift Reaction", *Catalysis Today*, Vol. 126, pp. 436-440.

Zalc, J. M., V. Sokolovskii, and D. G. Löffler, 2002, "Are Noble Metal-Based Water–Gas Shift Catalysts Practical for Automotive Fuel Processing?", *Journal of Catalysis*, Vol. 206, pp. 169-171.

Zheng, X., X. Zhang, X. Wang, S. Wang, and S. Wu, 2005, "Preparation and Characterization of CuO/CeO_2 Catalysts and Their Applications in Low-Temperature CO Oxidation", *Applied Catalysis A: General*, Vol. 295, pp. 142-149.